From X-ray Binaries to AGN

What do we learn from X-ray polarimetry?

Pierre-Olivier Petrucci, IPAG

Active Galactic Nuclei

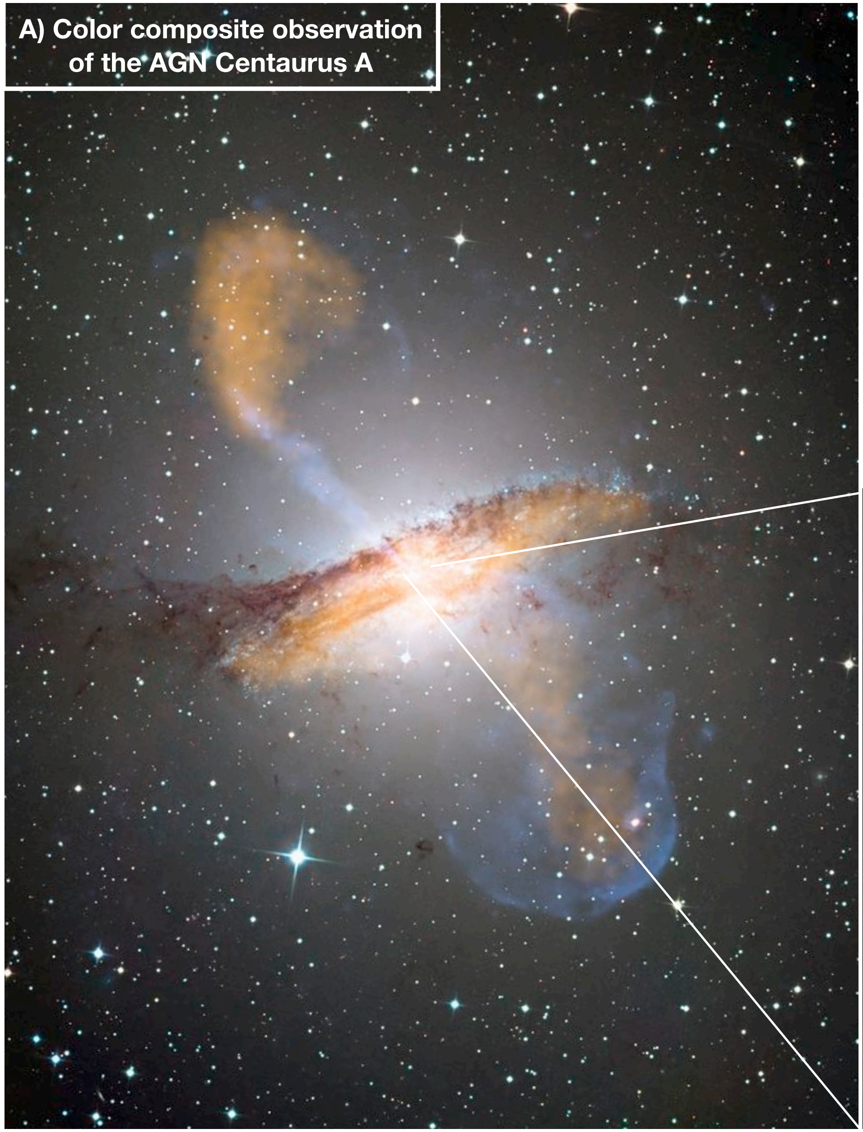

- 10% of the galaxies harbor a AGN in their center
- They are (roughly) divided into radio-quiet (no/weak jet) and radio-loud (jet) AGN
- Black hole mass

$$10^5 M_{sun} < M_{BH} < 10^{10} M_{sun}$$

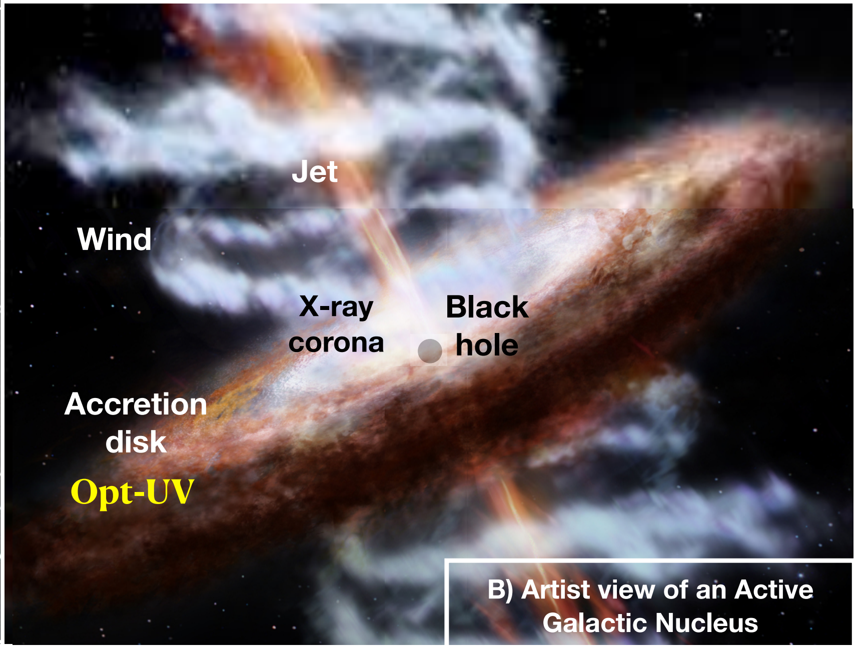

Black hole - Accretion disk - X-ray corona- Outflows

X-ray binaries

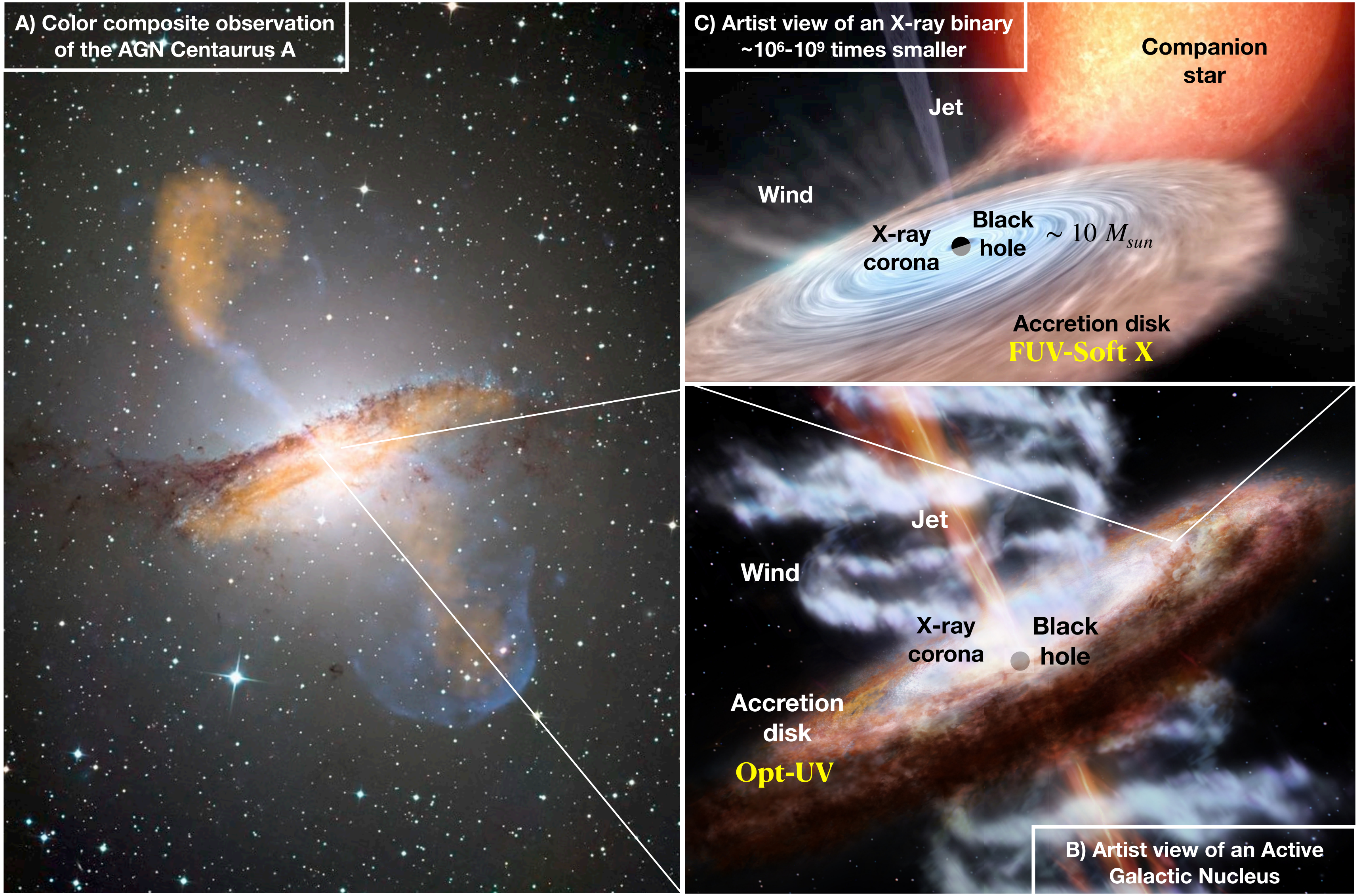

Black hole - Accretion disk - X-ray corona- Outflows

Same BH environment but different scales!

- Gravitational radius: $R_g = \frac{\mathcal{G}M_{BH}}{c^2} = 1.5 \times 10^5 \frac{M_{BH}}{M_{sun}}$cm

  ⇒15 km in a $10\ M_\odot$ BH ≡ 1 AU in a $10^8\ M_\odot$ BH

- Inner Stable Circular Orbit (ISCO): the smallest **marginally stable** circular orbit in which a test particle can stably orbit a massive object in general relativity

Reynolds (ARA&A 2021)

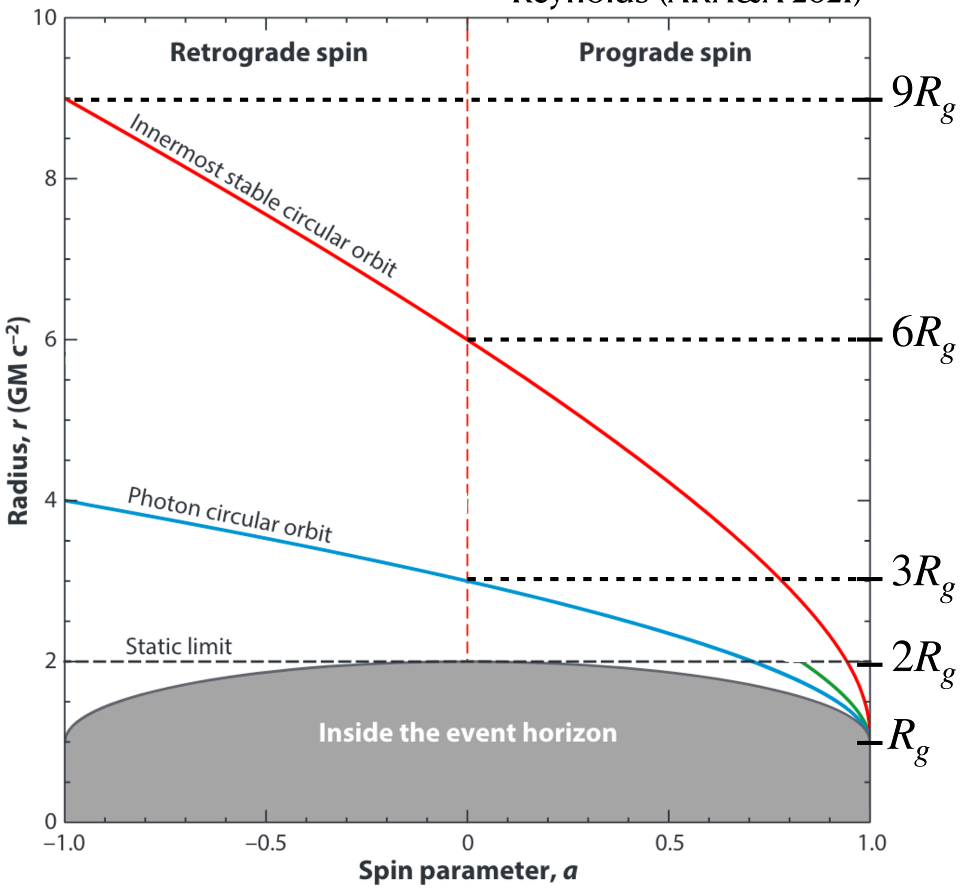

Same BH environment but different scales!

- Keplerian frequency at ISCO: $\Omega_K(R_{ISCO}) = \sqrt{\frac{GM_{BH}}{R^3_{ISCO}}} = \frac{c}{R_{ISCO}}\sqrt{\frac{R_g}{R_{ISCO}}}$

$$\Omega_K(R_{ISCO}) \simeq 10^4 Hz \text{ for a } 10\ M_\odot \text{ BH}$$

$$\Omega_K(R_{ISCO}) \simeq 10^{-3} Hz \text{ for a } 10^8\ M_\odot \text{ BH}$$

$\Rightarrow$ 10 ms in a $10\ M_\odot$ BH $\equiv$ 100 ks in a $10^8\ M_\odot$ BH

- Eddington luminosity: $L_{Edd} = \frac{4\pi \mathcal{G} M_{BH} m_p c}{\sigma_T} \simeq 1.3 \times 10^{38} \frac{M_{BH}}{M_\odot}$ erg s-1 (when emitted isotropically) would produce a radiative force on fully ionized hydrogen that balances gravity.

$\Rightarrow 3.4 \times 10^5 L_\odot$ in a $10\ M_\odot$ BH $\equiv$ $3.4 \times 10^{12} L_\odot$ in a $10^8\ M_\odot$ BH

Accretion disk

Shakura & Sunyaev (1973)   Reynolds (ARA&A 2021)

« Due to the angular momentum that infalling matter will inevitably possess, accreting matter will form a rotationally supported disk around the black hole. »

Assuming:

1. the system is in a steady state with an inward mass flux that is constant with radius (i.e., mass loss due to disk winds is negligible)
2. the accreting matter loses angular momentum via stresses internal to the disk (i.e., external torques due to a large-scale magnetic field are negligible)
3. the energy dissipated in the flow is radiated locally

$$T_{eff}(R) = 3.3 \times 10^7 \eta^{-1/4} \left(\frac{M}{10 M_\odot}\right)^{-1/4} \left(\frac{L}{L_{Edd}}\right)^{1/4} \left(\frac{R_g}{R}\right)^{3/4} \left(1 - \sqrt{\frac{R_{ISCO}}{R}}\right)^{1/4} \text{K}$$

with $\eta = \frac{L}{\dot{M} c^2}$ the « radiative efficicency » i.e. the efficiency with which accreting matter is converted into electromagnetic (EM) radiation

Accretion disk

Shakura & Sunyaev (1973) Reynolds (ARA&A 2021)

- Radiative efficiency η from ~10% for a=0 to 40% for a=1

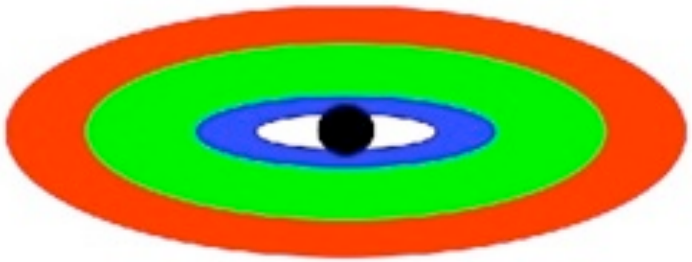

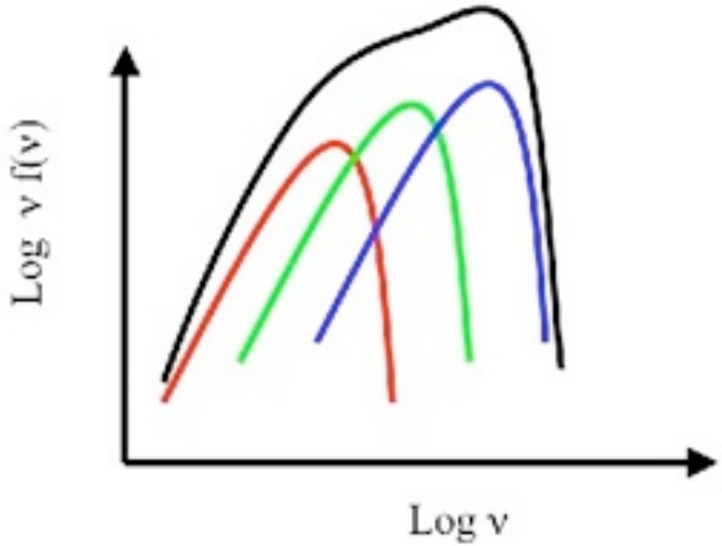

- $T_{\rm eff,max} = 6.16 \times 10^6 \eta^{-1/4} \left(\frac{M}{10\,{\rm M}_\odot}\right)^{-1/4} \left(\frac{L}{L_{\rm Edd}}\right)^{1/4} \left(\frac{r_{\rm isco}}{r_{\rm g}}\right)^{-3/4}$ K

- The larger the mass the cooler the disk. It radiates: **in UV for SMBH,**
  in soft X for 10 $M_\odot$ BH

X-ray bright sources

X-ray binaries

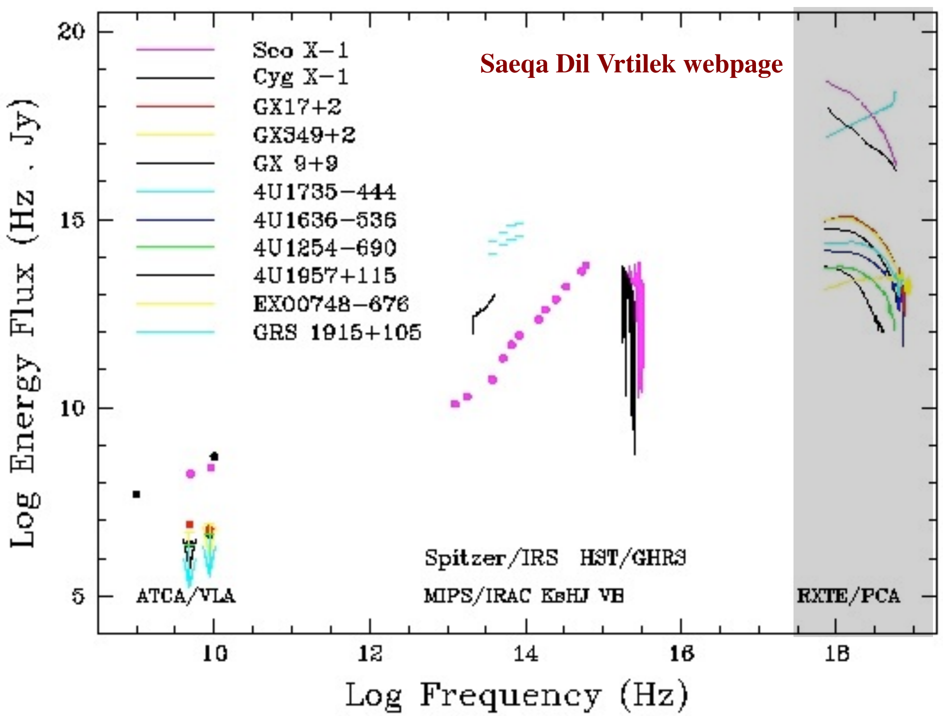

AGN

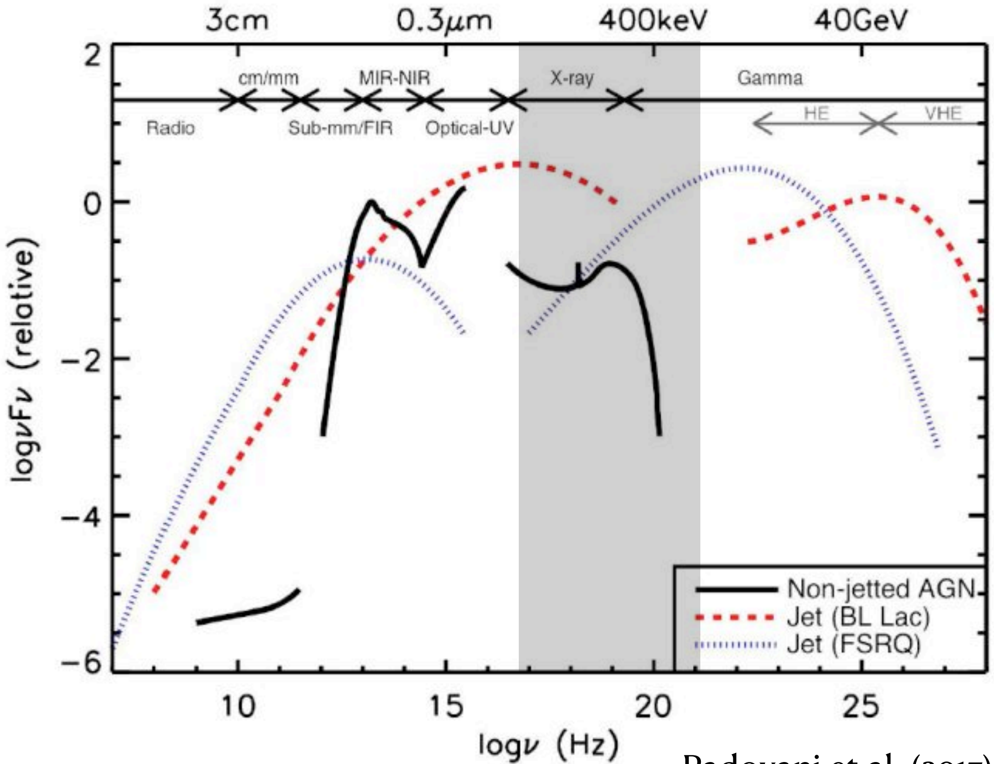

Padovani et al. (2017)

X-ray bright sources

X-ray binaries

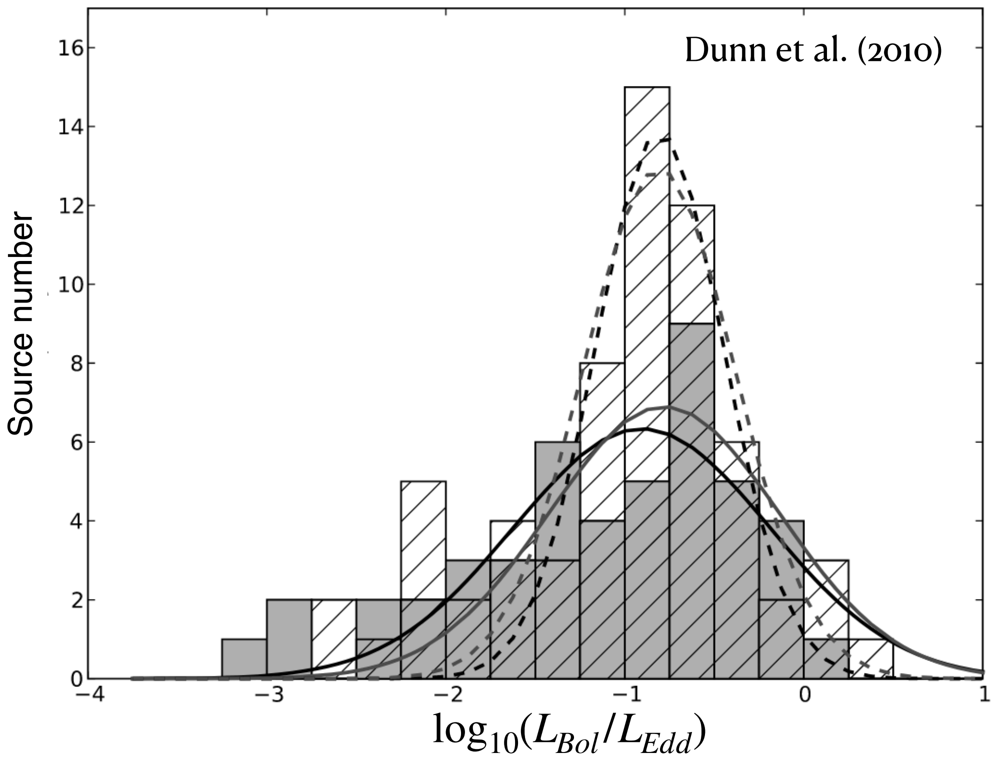

AGN

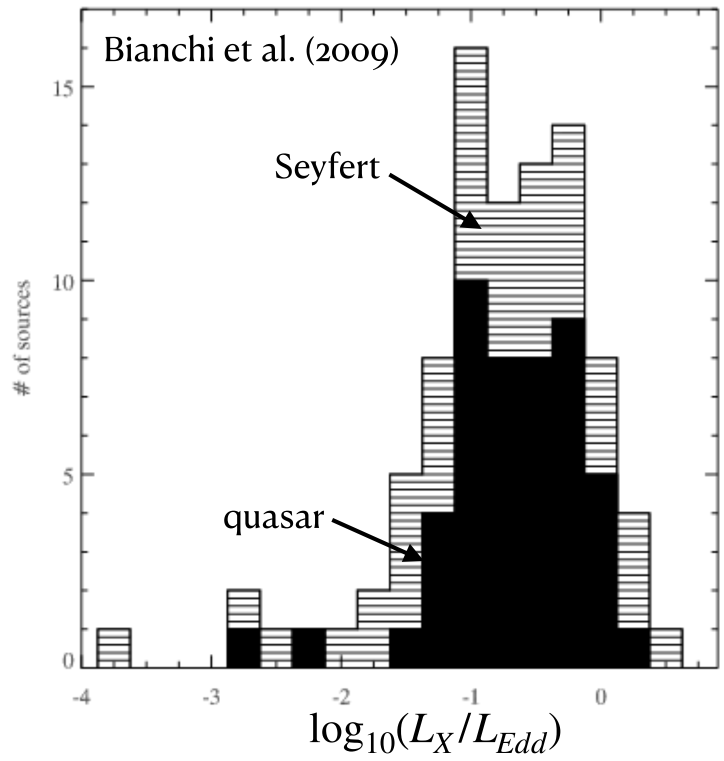

$$L_X \sim L_{bol} \sim 1 - 100\,\%\,L_{Edd}$$

But X-rays cannot be produced by the accretion disk….
need a hot plasma: the hot corona

Hot corona size

- Variability constraints: If the luminosity of an unresolved source varies significantly in a time scale ΔT, then the radius R_X of the source can be no larger than $c\Delta T$

- Observed variability of the order of the dynamical time scale (ms in XrB, hours in AGN)

$$R_X < c\Delta T \sim \text{few } R_g$$

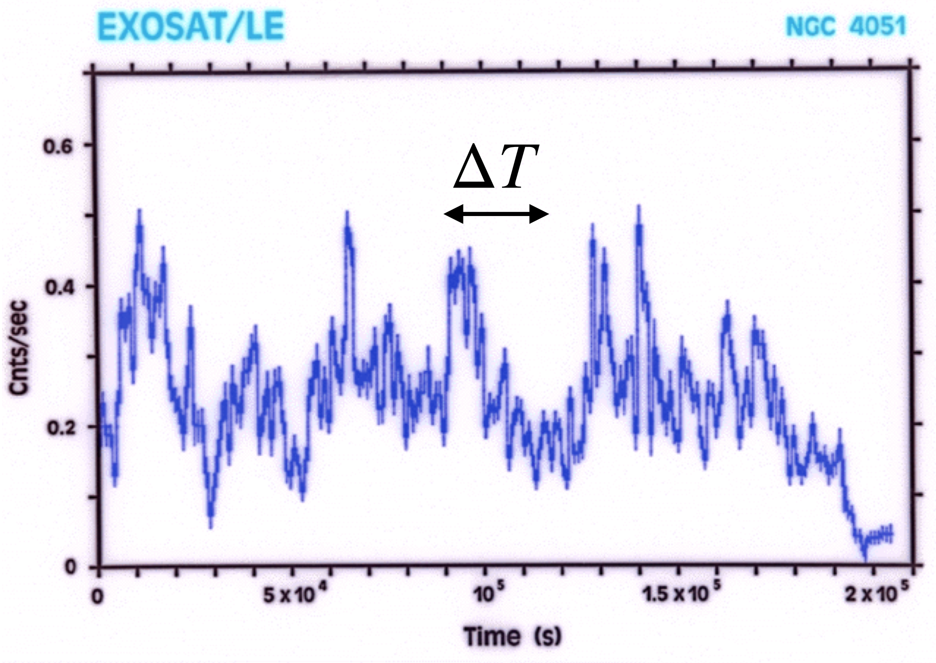

Hot corona size

- Microlensing

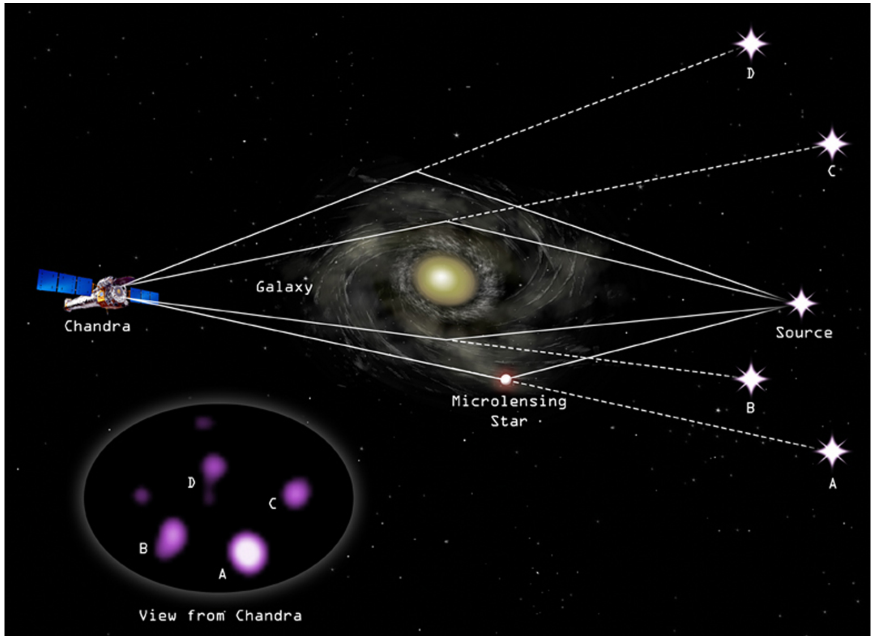

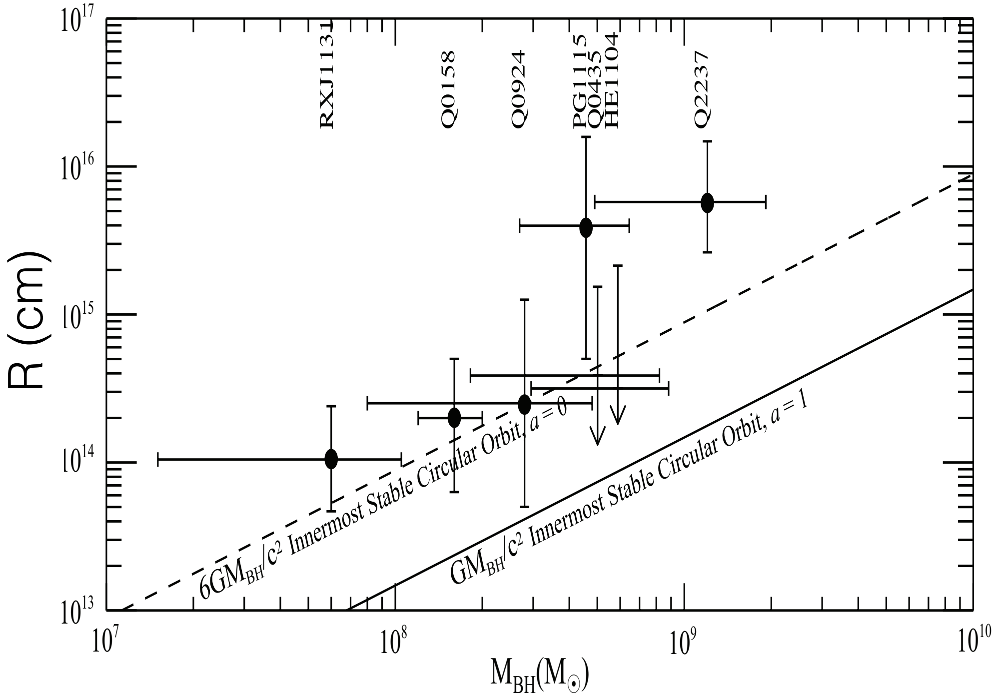

Chartas et al. (2016)

Estimates of the X-ray emitting region size from variability of the different lensed images

Hot corona emission

It shows a cut-off power law shape

AGN

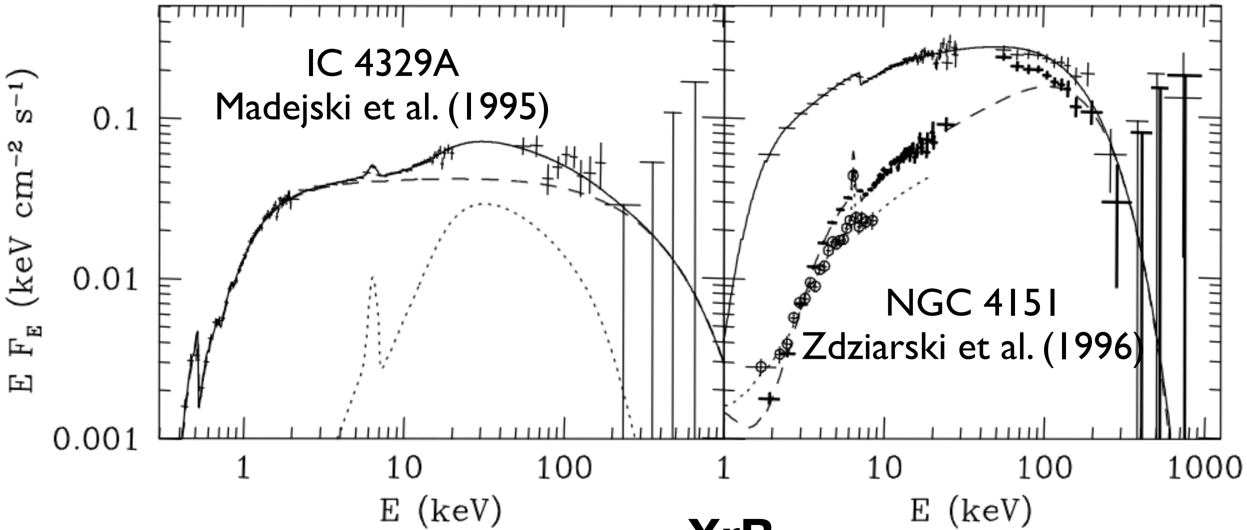

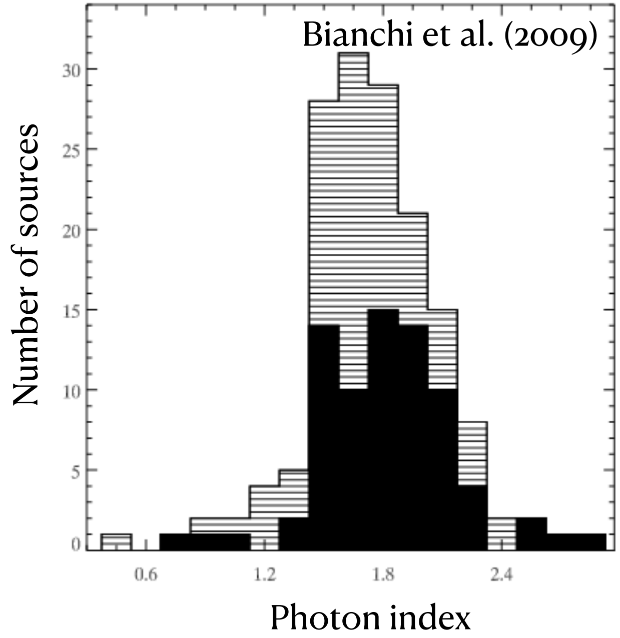

XrB

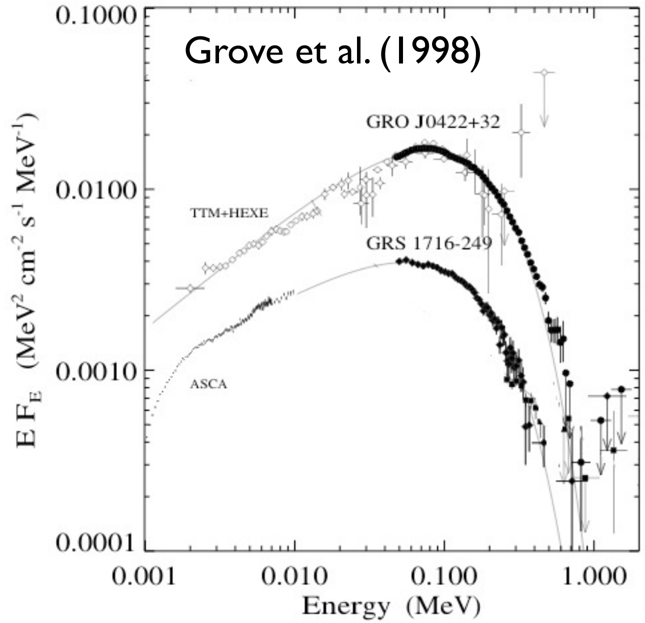

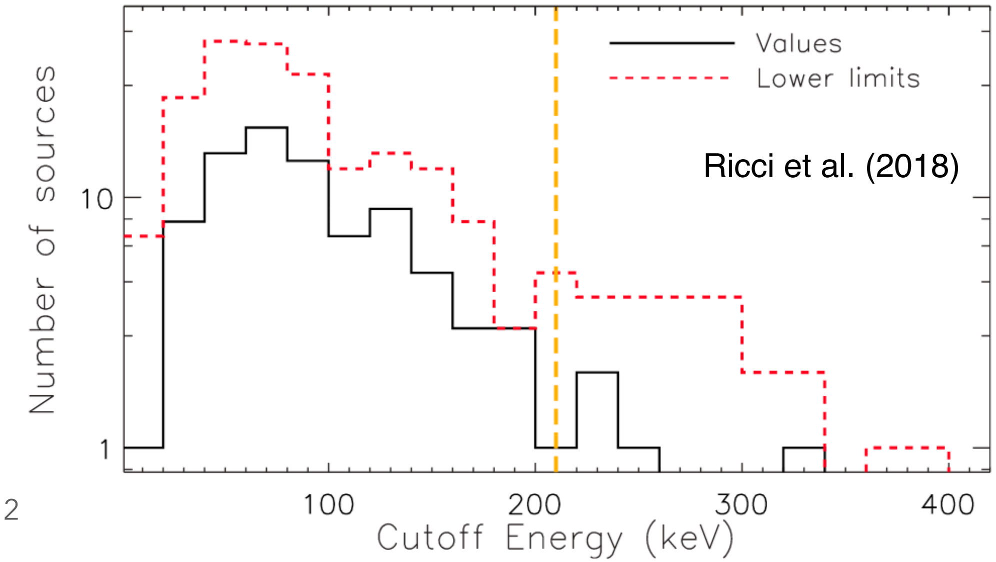

Hot corona radiative process

- Cut-off power law shape well explains by thermal comptonisation on surrounding photons (=from the accretion disk)

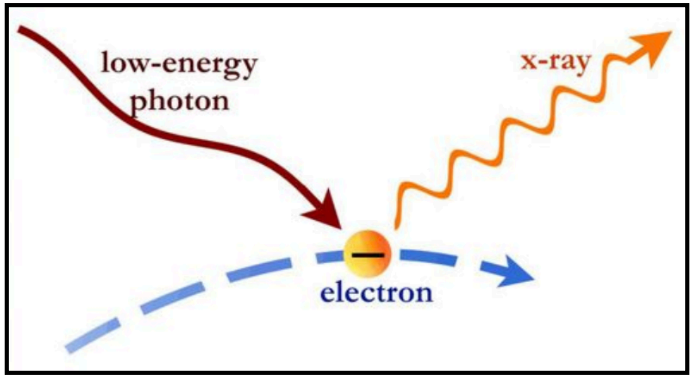

Hot corona radiative process

- Cut-off power law shape well explains by thermal comptonisation on surrounding photons (=from the accretion disk)

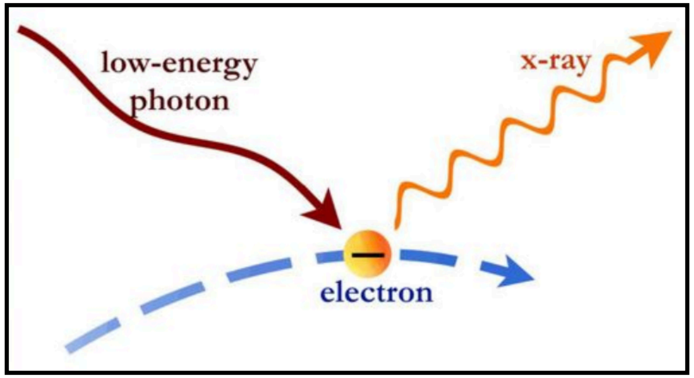

- For thermal plasma with electron temperature T_e and optical depth $\boldsymbol{\tau}$

Mean change in energy per scatterings:

$$\frac{\Delta E}{E} = \frac{4kT_e}{m_e c^2} + 16\left(\frac{kT_e}{m_e c^2}\right)^2$$

Mean number of scatterings:

$$N \simeq (\tau + \tau^2)$$

Mean probability of being scattered:

$$P \simeq (1 - e^{-\tau})$$

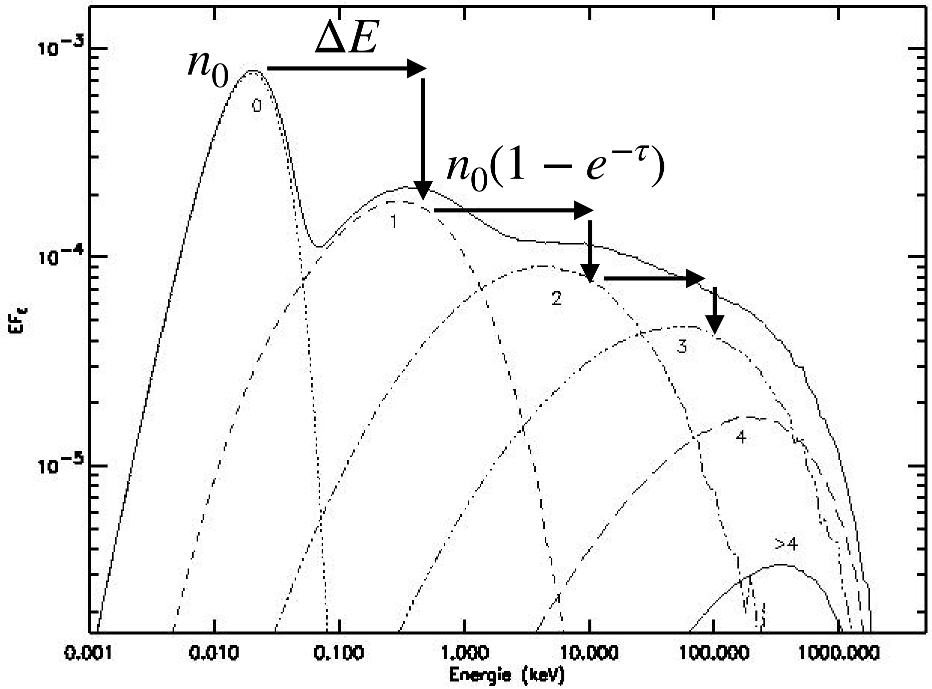

Hot corona radiative process

•Cut-off power law shape well explains by thermal comptonisation on surrounding photons (=from the accretion disk)

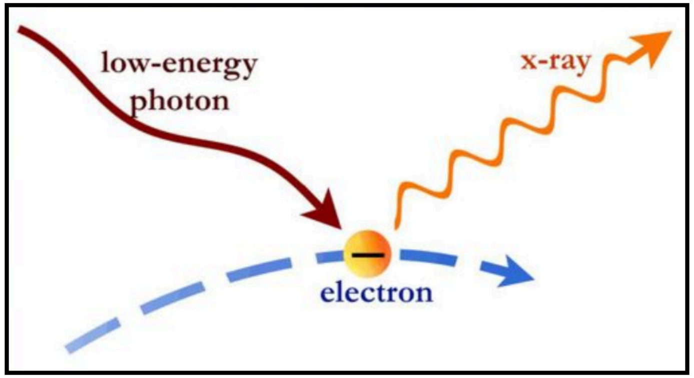

• For thermal plasma with electron temperature T_e and optical depth $\boldsymbol{\tau}$

For $E \gg E_0$, the spectral shape is generally approximated by a cut-off power law shape:

$$F_E \propto E^{-\Gamma} \exp\left(-\frac{E}{E_c}\right)$$

with $\Gamma(T_e,\tau)$ and $Ec(T_e,\tau)$

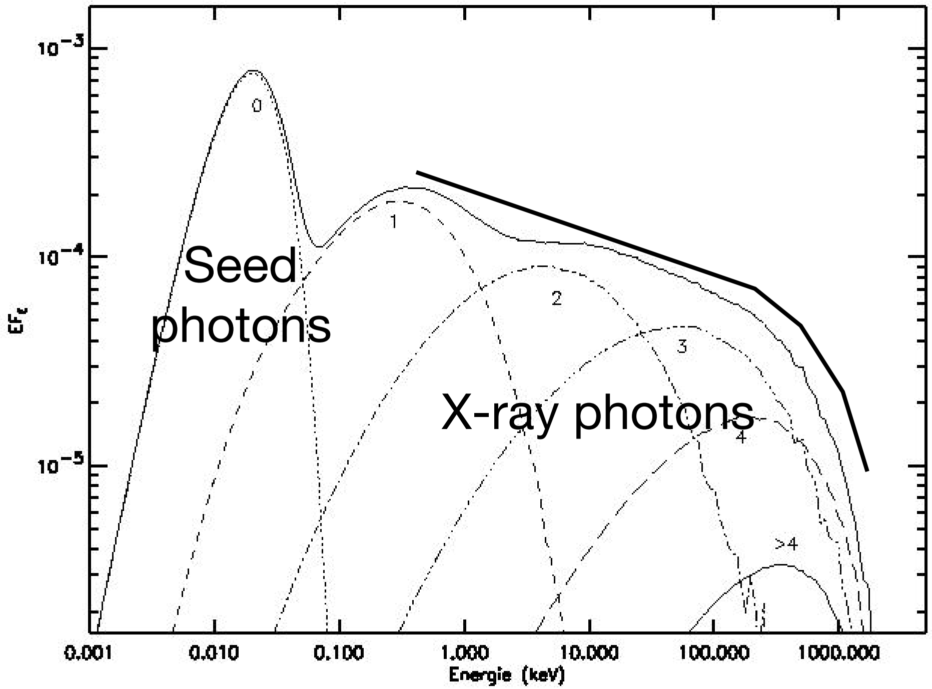

Disk-corona structure

NGC 5548 Connolly et al. (2015)

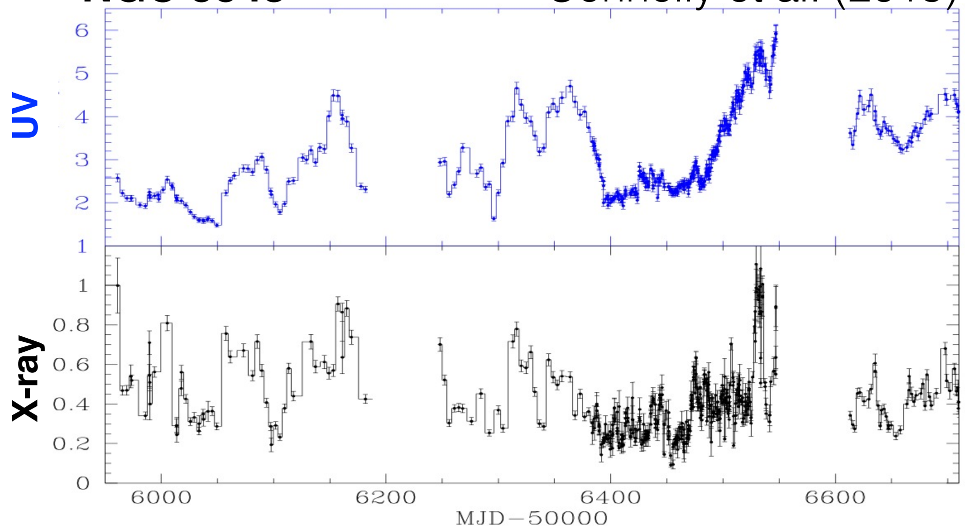

NGC 2617 Shappee et al. (2014)

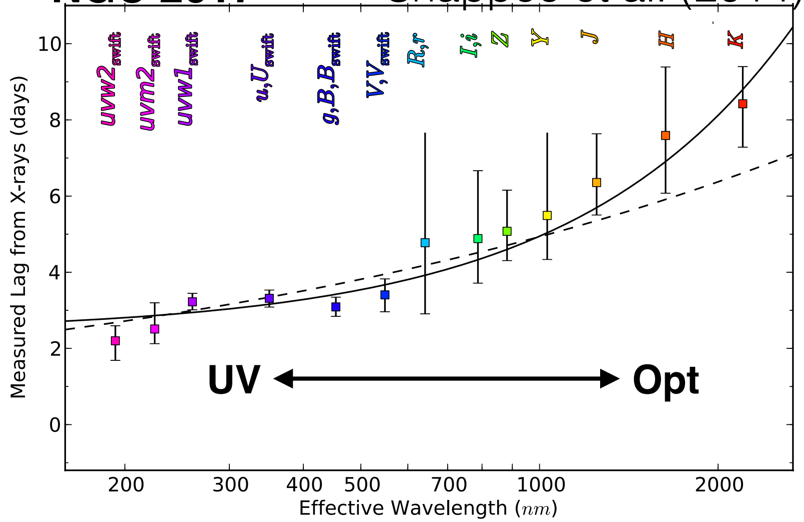

Quasi-simultaneity X-ray/UV

➪ **Distance X/UV < light days (100s Rg)**

Hot corona-Disk Geometry

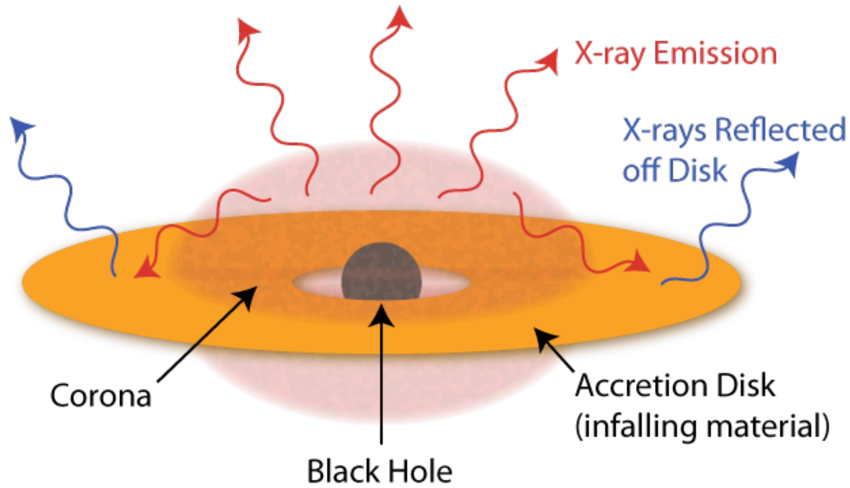

?

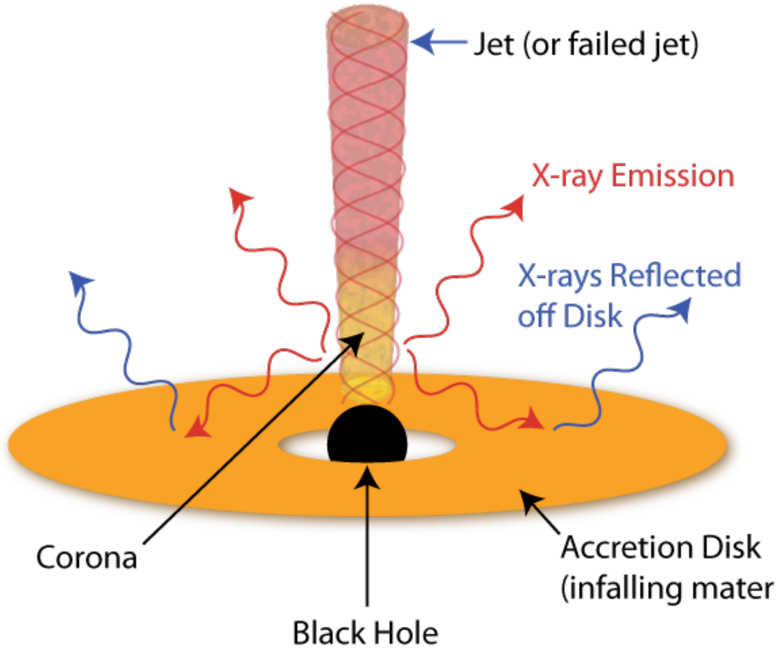

Inner part of the accretion flow

Above the BH (base of the jet?)

Radiative Equilibrium

Whatever the geometry, a radiative interaction is expected (e.g., Haardt & Maraschi 1991)

- UV from the accretion disk cool the hot corona via Compton Scattering
- X-rays from the hot corona heat the accretion disk via illumination

Radiative Equilibrium

Whatever the geometry, a radiative interaction is expected (e.g., Haardt & Maraschi 1991)

- UV from the accretion disk cool the hot corona via Compton Scattering
- X-rays from the hot corona heat the accretion disk via illumination

➡ Γ, kT_e and τ_c are linked one with each other

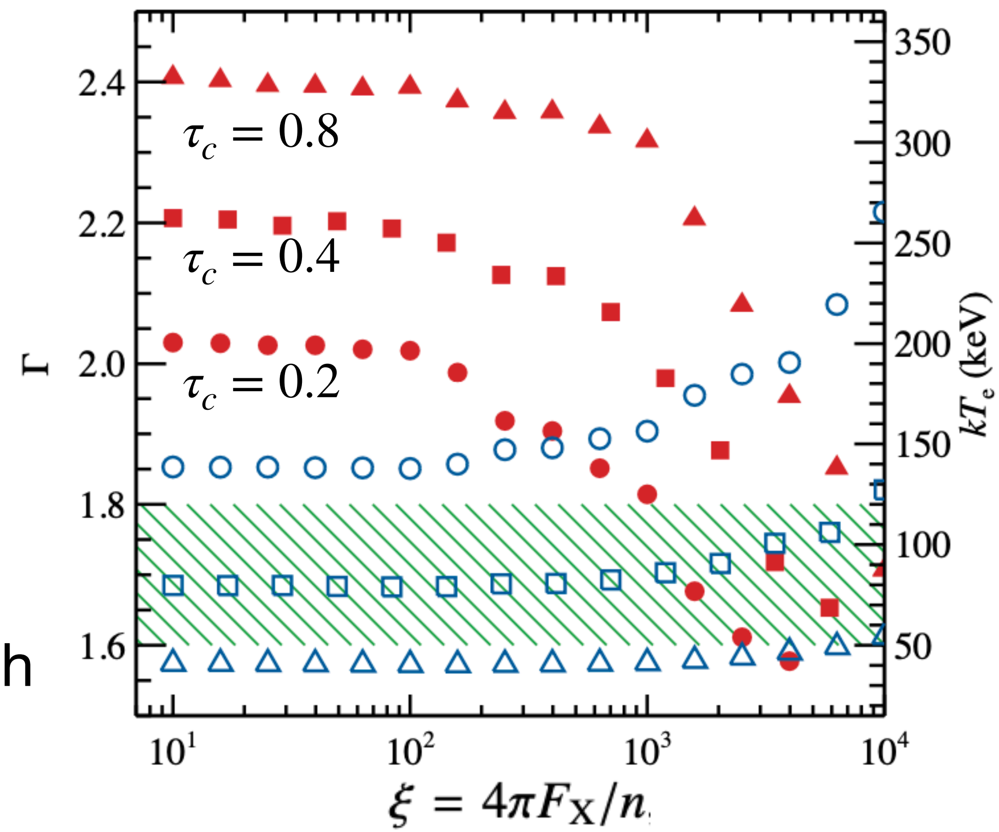

Malzac et al. (2001), Poutanen et al. (2018)

Radiative Equilibrium

Whatever the geometry, a radiative interaction is expected (e.g., Haardt & Maraschi 1991)

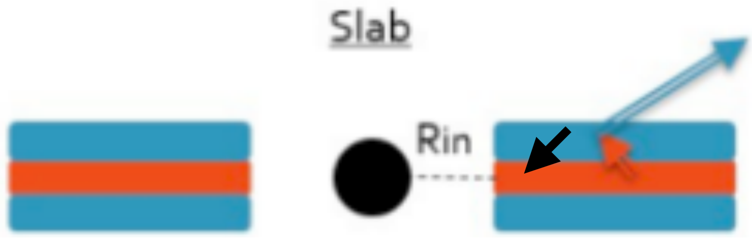

- UV from the accretion disk cool the hot corona via Compton Scattering
- X-rays from the hot corona heat the accretion disk via illumination

➡ Γ, kT_e and τ_c are linked one with each other

➡**But spectral fits not able to discriminate**

NGC 5548

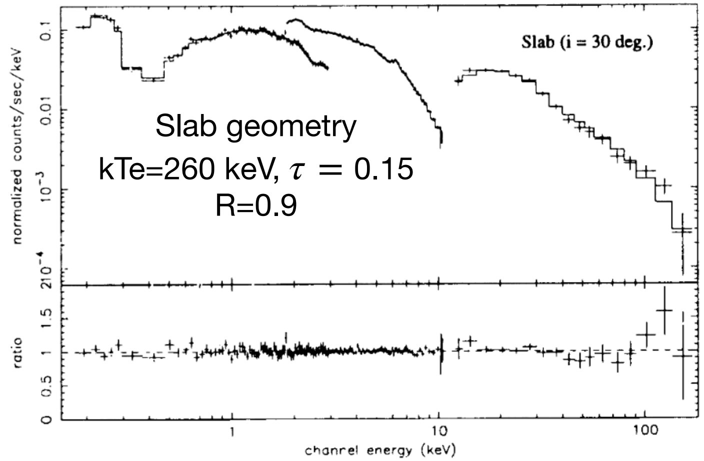

Petrucci et al. (2001)

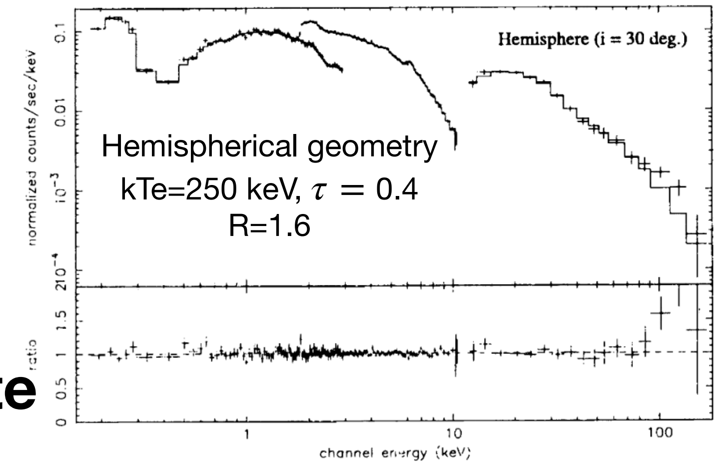

X-ray Polarimetry: opening of a new era

IXPE : Imaging X-ray Polarimetry Explorer

- NASA/SMEX
- spectroscopie, imagerie, timing et polarimétrie (2-8 keV)
- 325 kg
- 160 millions dollars
- Launched 9 Dec 2021

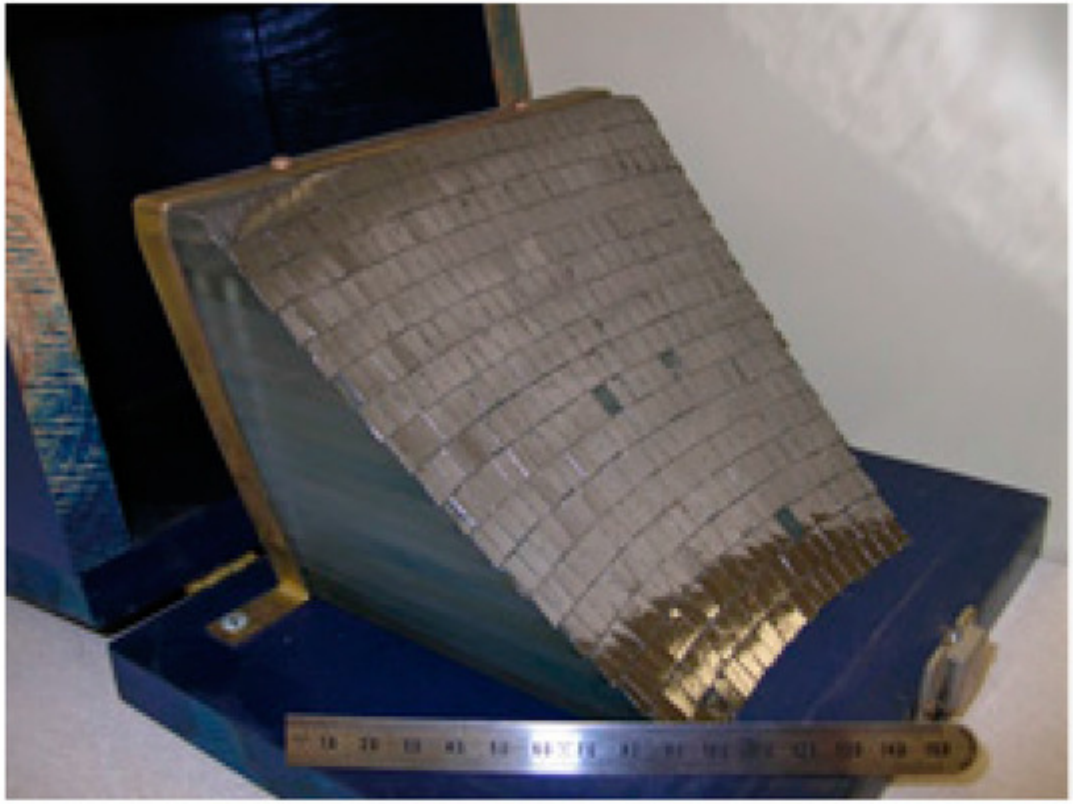

Graphite Cristal detector in OSO-8 1975-1978 (Weisskopf 2018)

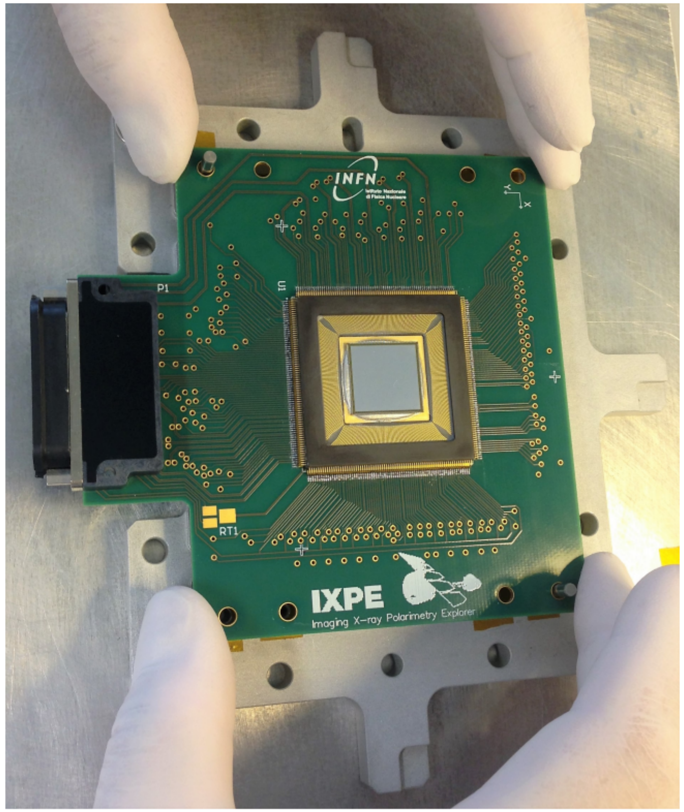

Gas Pixel Detector (Sgrò et al. 2017)

X-ray Polarimetry: opening of a new era

IXPE : Imaging X-ray Polarimetry Explorer

- NASA/SMEX
- spectroscopie, imagerie, timing et polarimétrie (2-8 keV)
- 325 kg
- 160 millions dollars
- Launched 9 Dec 2021

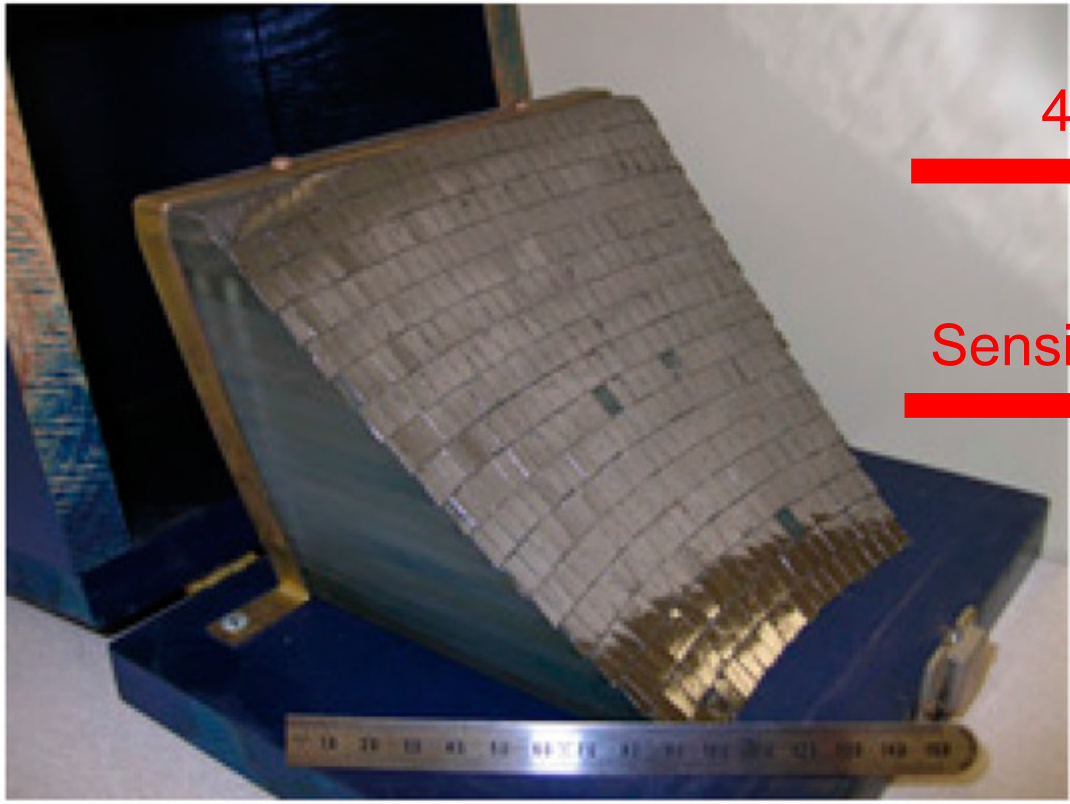

40 years

Sensitivity x100

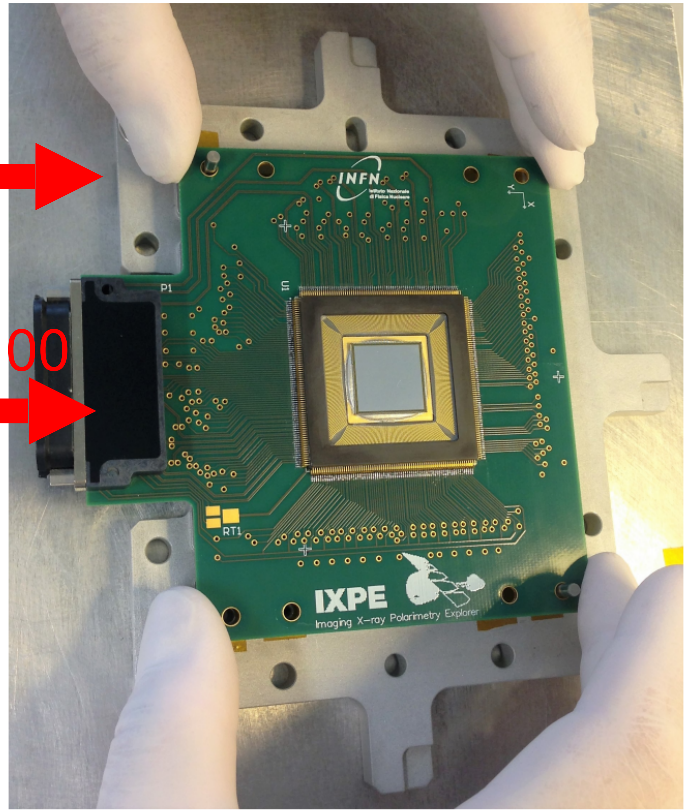

Graphite Cristal detector in OSO-8 1975-1978 (Weisskopf 2018)

GPD (Sgrò et al. 2017)

X-ray Polarimetry: opening of a new era

IXPE : Imaging X-ray Polarimetry Explorer

- NASA/SMEX
- spectroscopie, imagerie, timing et polarimétrie (2-8 keV)
- 325 kg
- 160 millions dollars
- Launched 9 Dec 2021

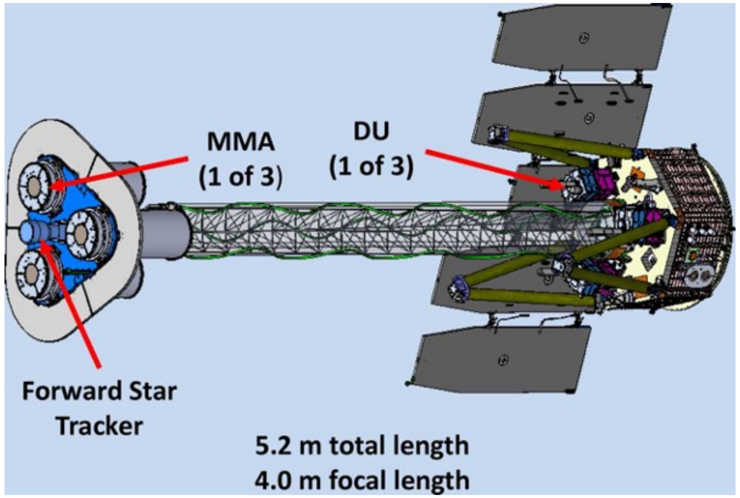

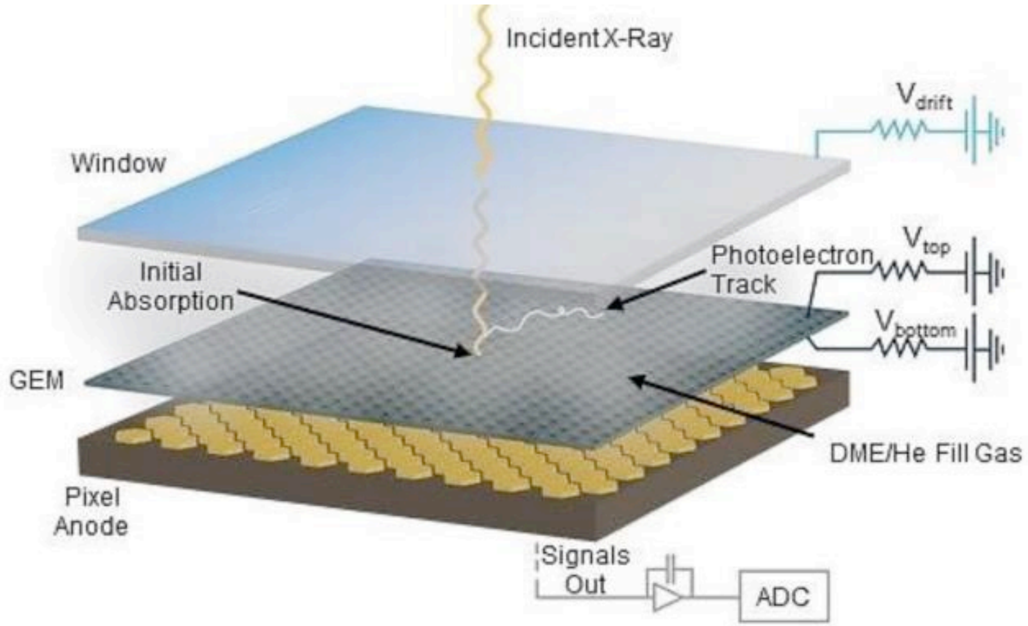

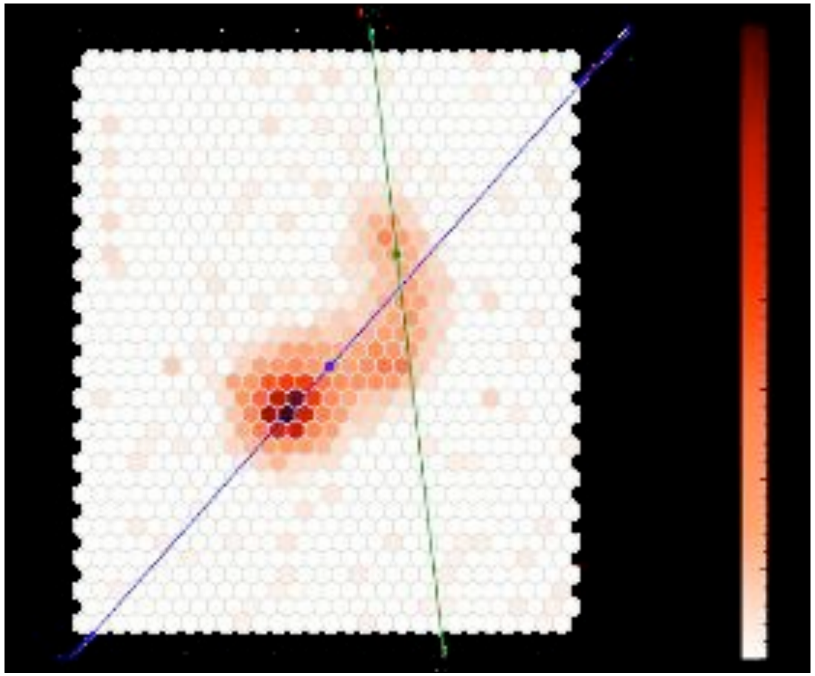

The distribution of initial photoelectron directions determines the degree and angle of polarization.

Characteristics and Target List

Parameter	Performance
Launch mass	330 kg
Length	5.2 m (deployed)
Nominal lifetime	2 years (no life-limiting consumables)
Energy band	2 to 8 keV
FOV (detector limited)	12.9 arcmin square
half-power diameter	28 arcsec @ 4.5 keV
Effective area per mirror module (x3)	166 cm^2 @ 2.3 keV
Energy resolution (FWHM)	0.52 keV @ 2 keV ($\propto \sqrt{E}$)
Timing	1 μs

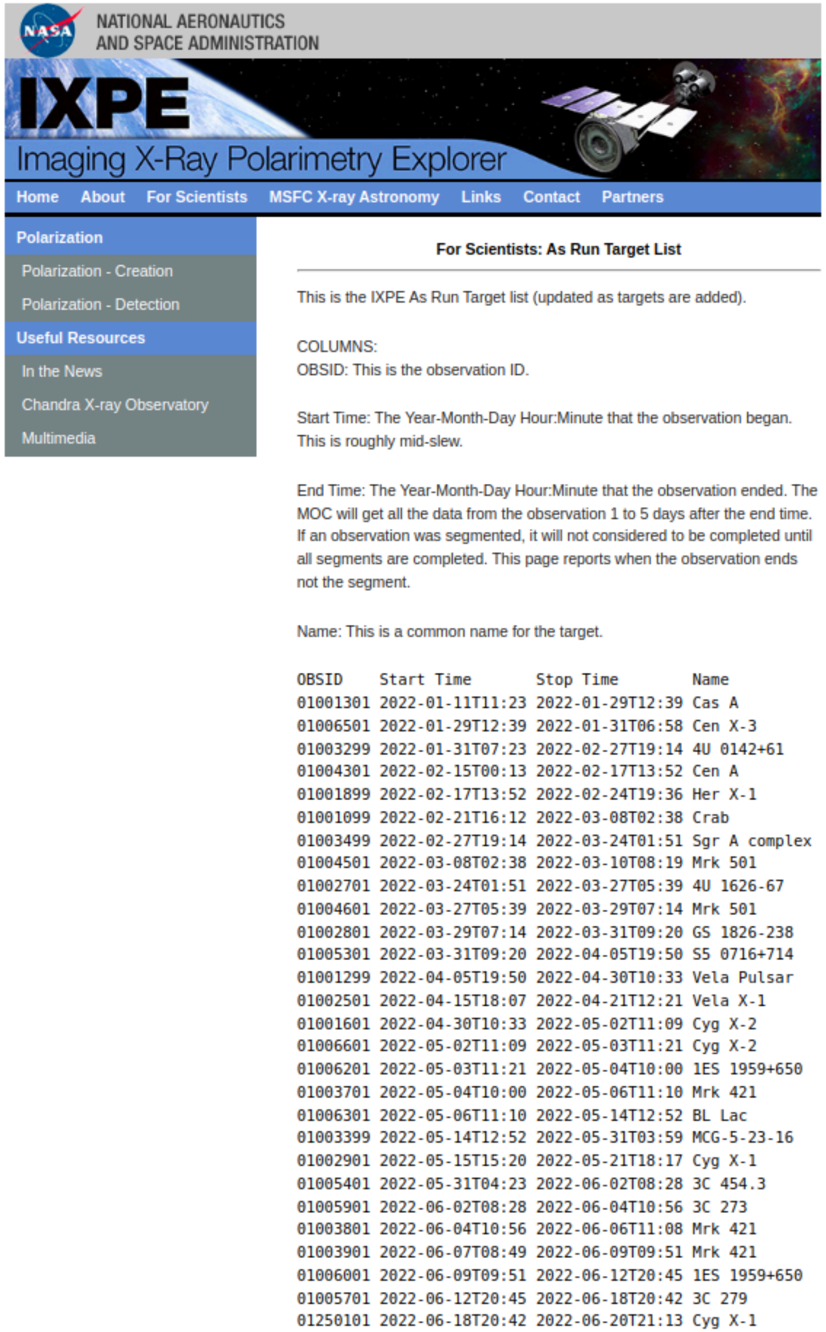
NATIONAL AERONAUTICS AND SPACE ADMINISTRATION

IXPE

Imaging X-Ray Polarimetry Explorer

Home | About | For Scientists | MSFC X-ray Astronomy | Links | Contact | Partners

Polarization
- Polarization - Creation
- Polarization - Detection

Useful Resources
- In the News
- Chandra X-ray Observatory
- Multimedia

For Scientists: As Run Target List

This is the IXPE As Run Target list (updated as targets are added).

COLUMNS:
OBSID: This is the observation ID.

Start Time: The Year-Month-Day Hour:Minute that the observation began. This is roughly mid-slew.

End Time: The Year-Month-Day Hour:Minute that the observation ended. The MOC will get all the data from the observation 1 to 5 days after the end time. If an observation was segmented, it will not considered to be completed until all segments are completed. This page reports when the observation ends not the segment.

Name: This is a common name for the target.

OBSID	Start Time	Stop Time	Name
01001301	2022-01-11T11:23	2022-01-29T12:39	Cas A
01006501	2022-01-29T12:39	2022-01-31T06:58	Cen X-3
01003299	2022-01-31T07:23	2022-02-27T19:14	4U 0142+61
01004301	2022-02-15T00:13	2022-02-17T13:52	Cen A
01001899	2022-02-17T13:52	2022-02-24T19:36	Her X-1
01001099	2022-02-21T16:12	2022-03-08T02:38	Crab
01003499	2022-02-27T19:14	2022-03-24T01:51	Sgr A complex
01004501	2022-03-08T02:38	2022-03-10T08:19	Mrk 501
01002701	2022-03-24T01:51	2022-03-27T05:39	4U 1626-67
01004601	2022-03-27T05:39	2022-03-29T07:14	Mrk 501
01002801	2022-03-29T07:14	2022-03-31T09:20	GS 1826-238
01005301	2022-03-31T09:20	2022-04-05T19:50	S5 0716+714
01001299	2022-04-05T19:50	2022-04-30T10:33	Vela Pulsar
01002501	2022-04-15T18:07	2022-04-21T12:21	Vela X-1
01001601	2022-04-30T10:33	2022-05-02T11:09	Cyg X-2
01006601	2022-05-02T11:09	2022-05-03T11:21	Cyg X-2
01006201	2022-05-03T11:21	2022-05-04T10:00	1ES 1959+650
01003701	2022-05-04T10:00	2022-05-06T11:10	Mrk 421
01006301	2022-05-06T11:10	2022-05-14T12:52	BL Lac
01003399	2022-05-14T12:52	2022-05-31T03:59	MCG-5-23-16
01002901	2022-05-15T15:20	2022-05-21T18:17	Cyg X-1
01005401	2022-05-31T04:23	2022-06-02T08:28	3C 454.3
01005901	2022-06-02T08:28	2022-06-04T10:56	3C 273
01003801	2022-06-04T10:56	2022-06-06T11:08	Mrk 421
01003901	2022-06-07T08:49	2022-06-09T09:51	Mrk 421
01006001	2022-06-09T09:51	2022-06-12T20:45	1ES 1959+650
01005701	2022-06-12T20:45	2022-06-18T20:42	3C 279
01250101	2022-06-18T20:42	2022-06-20T21:13	Cyg X-1

Characteristics and Target List

Parameter	Performance
Launch mass	330 kg
Length	5.2 m (deployed)
Nominal lifetime	2 years (no life-limiting consumables)
Energy band	2 to 8 keV
FOV (detector limited)	12.9 arcmin square
half-power diameter	28 arcsec @ 4.5 keV
Effective area per mirror module (x3)	166 cm² @ 2.3 keV
Energy resolution (FWHM)	0.52 keV @ 2 keV ($\propto \sqrt{E}$)
Timing	1 µs

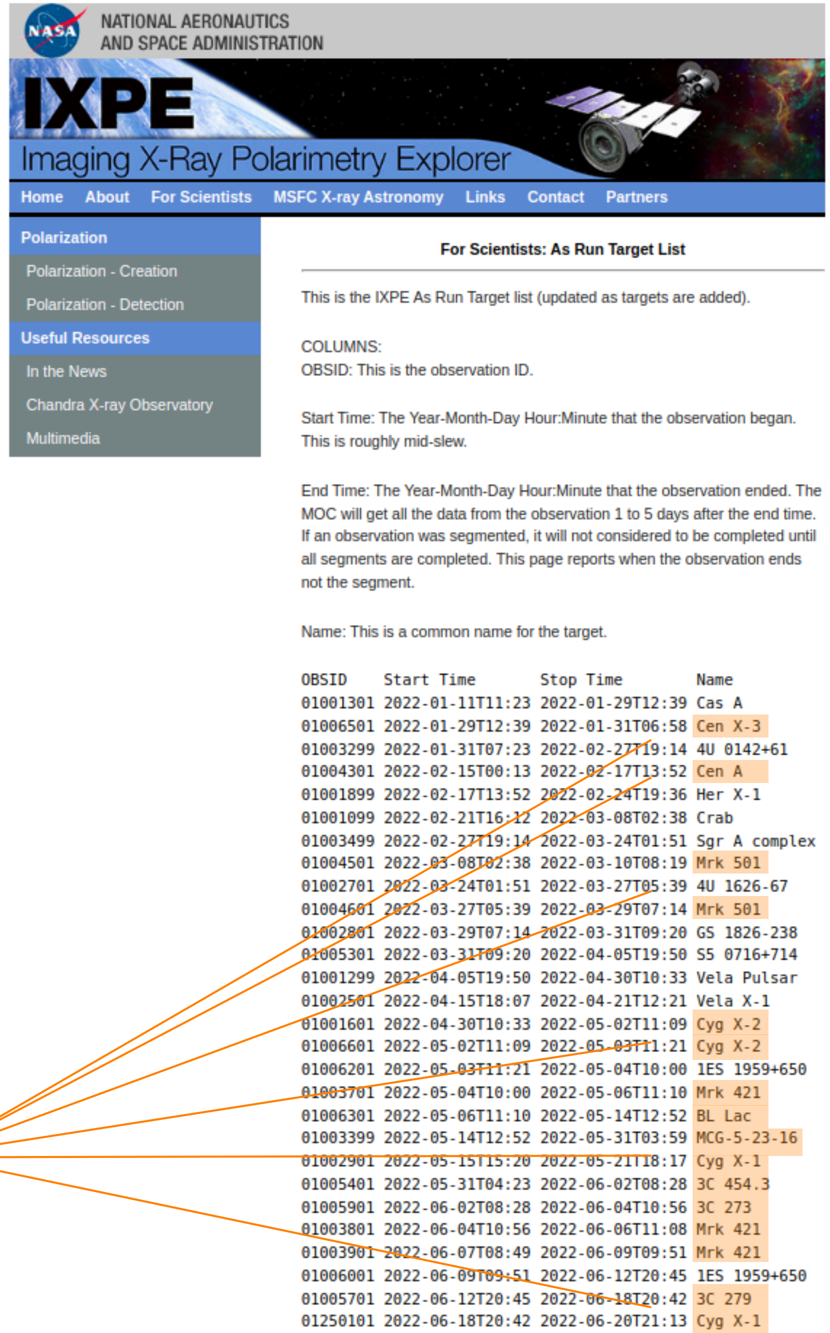
NATIONAL AERONAUTICS AND SPACE ADMINISTRATION

IXPE

Imaging X-Ray Polarimetry Explorer

Home | About | For Scientists | MSFC X-ray Astronomy | Links | Contact | Partners

Polarization
- Polarization - Creation
- Polarization - Detection

Useful Resources
- In the News
- Chandra X-ray Observatory
- Multimedia

For Scientists: As Run Target List

This is the IXPE As Run Target list (updated as targets are added).

COLUMNS:
OBSID: This is the observation ID.

Start Time: The Year-Month-Day Hour:Minute that the observation began. This is roughly mid-slew.

End Time: The Year-Month-Day Hour:Minute that the observation ended. The MOC will get all the data from the observation 1 to 5 days after the end time. If an observation was segmented, it will not considered to be completed until all segments are completed. This page reports when the observation ends not the segment.

Name: This is a common name for the target.

OBSID	Start Time	Stop Time	Name
01001301	2022-01-11T11:23	2022-01-29T12:39	Cas A
01006501	2022-01-29T12:39	2022-01-31T06:58	Cen X-3
01003299	2022-01-31T07:23	2022-02-27T19:14	4U 0142+61
01004301	2022-02-15T00:13	2022-02-17T13:52	Cen A
01001899	2022-02-17T13:52	2022-02-24T19:36	Her X-1
01001099	2022-02-21T16:12	2022-03-08T02:38	Crab
01003499	2022-02-27T19:14	2022-03-24T01:51	Sgr A complex
01004501	2022-03-08T02:38	2022-03-10T08:19	Mrk 501
01002701	2022-03-24T01:51	2022-03-27T05:39	4U 1626-67
01004601	2022-03-27T05:39	2022-03-29T07:14	Mrk 501
01002801	2022-03-29T07:14	2022-03-31T09:20	GS 1826-238
01005301	2022-03-31T09:20	2022-04-05T19:50	S5 0716+714
01001299	2022-04-05T19:50	2022-04-30T10:33	Vela Pulsar
01002501	2022-04-15T18:07	2022-04-21T12:21	Vela X-1
01001601	2022-04-30T10:33	2022-05-02T11:09	Cyg X-2
01006601	2022-05-02T11:09	2022-05-03T11:21	Cyg X-2
01006201	2022-05-03T11:21	2022-05-04T10:00	1ES 1959+650
01003701	2022-05-04T10:00	2022-05-06T11:10	Mrk 421
01006301	2022-05-06T11:10	2022-05-14T12:52	BL Lac
01003399	2022-05-14T12:52	2022-05-31T03:59	MCG-5-23-16
01002901	2022-05-15T15:20	2022-05-21T18:17	Cyg X-1
01005401	2022-05-31T04:23	2022-06-02T08:28	3C 454.3
01005901	2022-06-02T08:28	2022-06-04T10:56	3C 273
01003801	2022-06-04T10:56	2022-06-06T11:08	Mrk 421
01003901	2022-06-07T08:49	2022-06-09T09:51	Mrk 421
01006001	2022-06-09T09:51	2022-06-12T20:45	1ES 1959+650
01005701	2022-06-12T20:45	2022-06-18T20:42	3C 279
01250101	2022-06-18T20:42	2022-06-20T21:13	Cyg X-1

Binaires X et AGNs

First AO (deadline 18th of Oct.)!

Hot corona -Disk Geometry

Constraint from X-ray polarisation

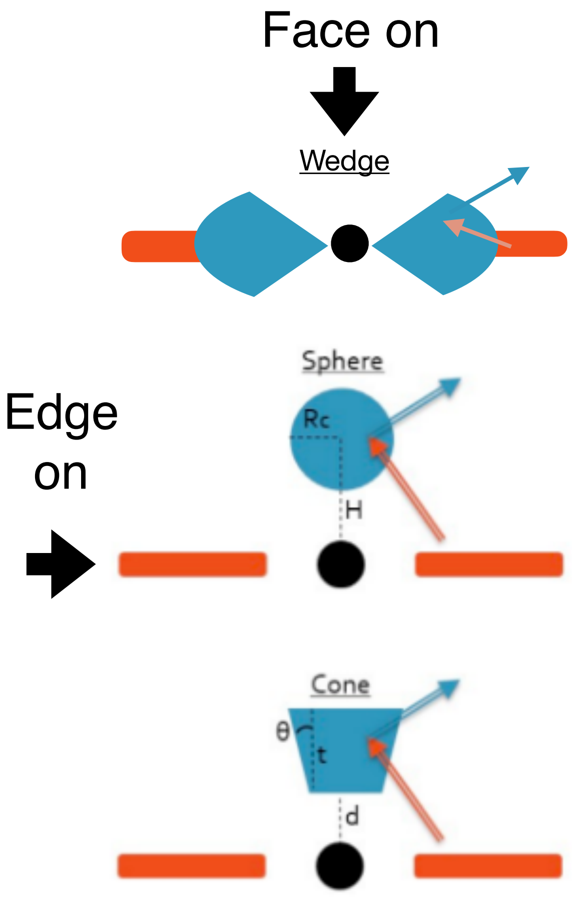

Ursini et al. (2022)

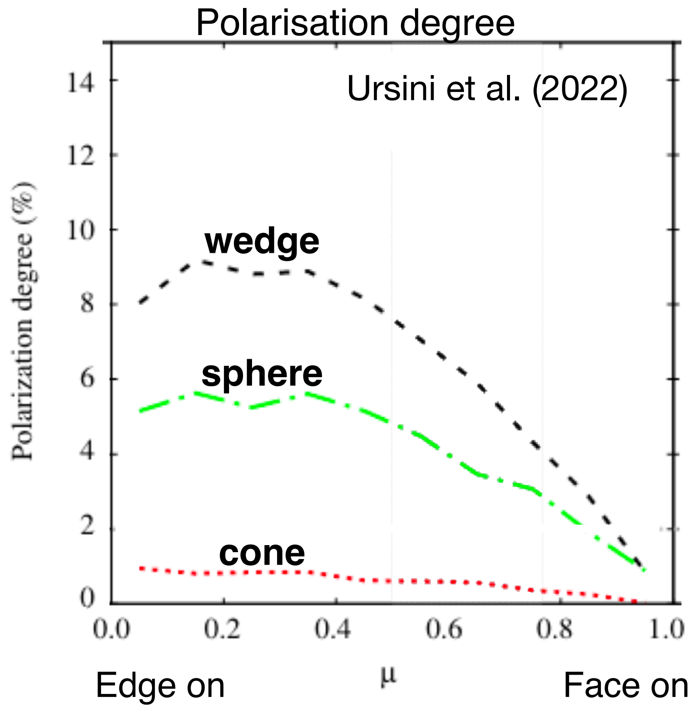

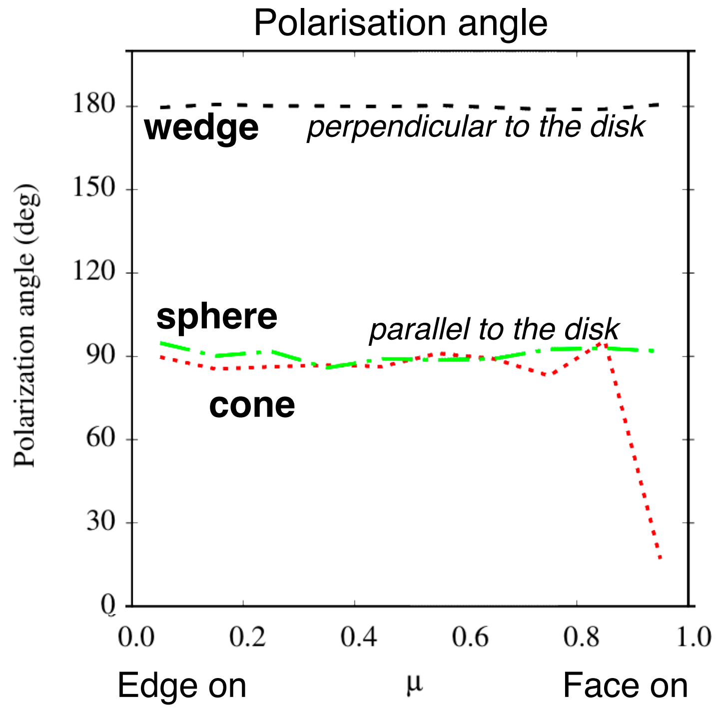

Wedge: high X-ray polarimetry, perpendicular to the disk

Sphere/cone: low X-ray polarimetry, perpendicular to the disk

The Case of the Microquasar Cygnus X-1

Observation IXPE

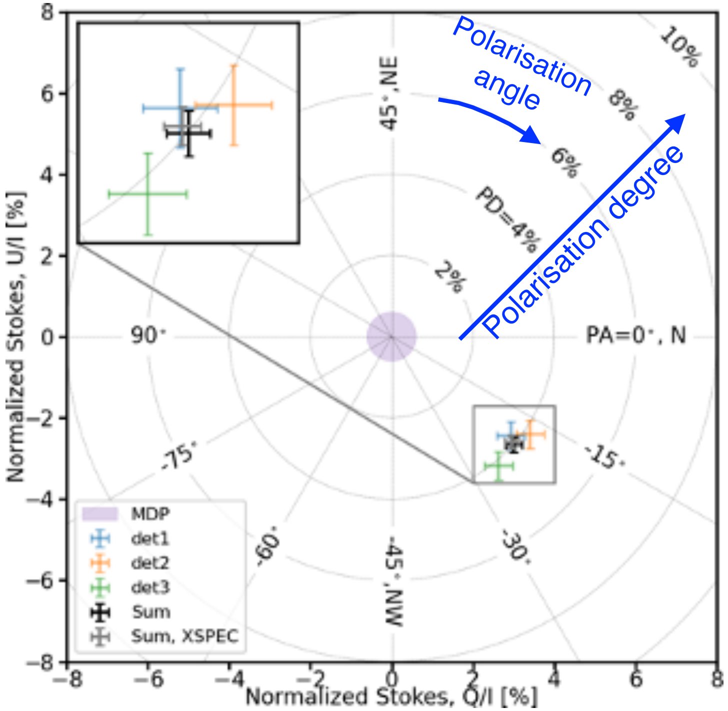

Krawczynski et al. (2022)

- Polarisation of ~ 4%, polarisation angle of ~-20 deg

The Case of the Microquasar Cygnus X-1

Observation IXPE

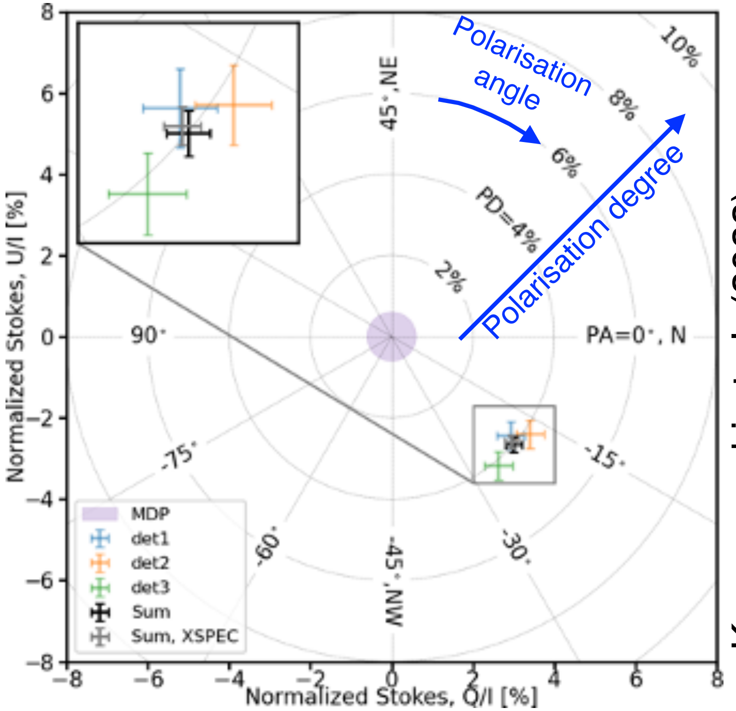

Krawczynski et al. (2022)

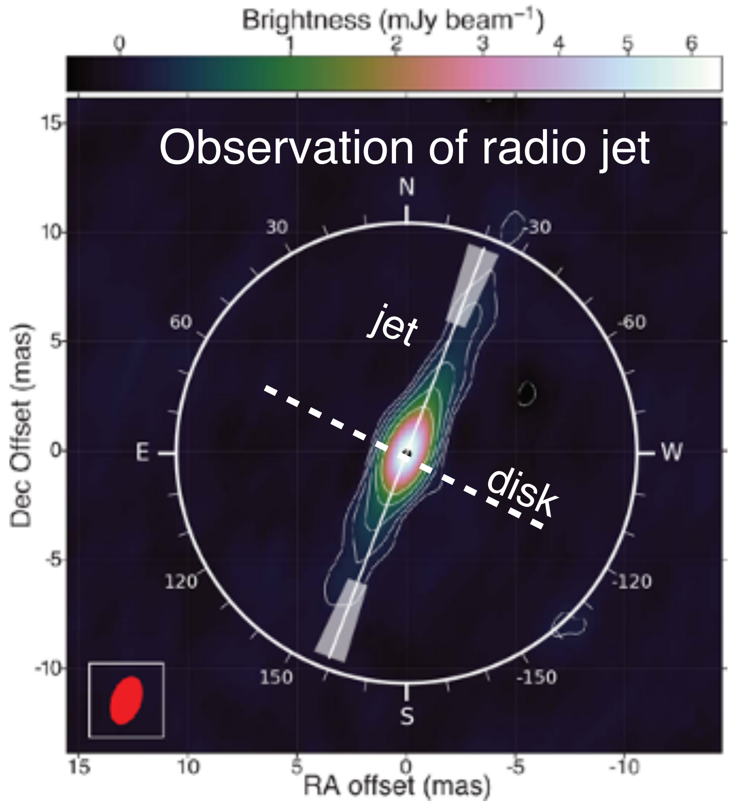

- Polarisation of ~ 4%, polarisation angle of ~-20 deg

➡ Polarisation angle parallel to the radio jet, i.e., perpendicular to the accretion disk

The Case of the Microquasar Cygnus X-1

Observation IXPE

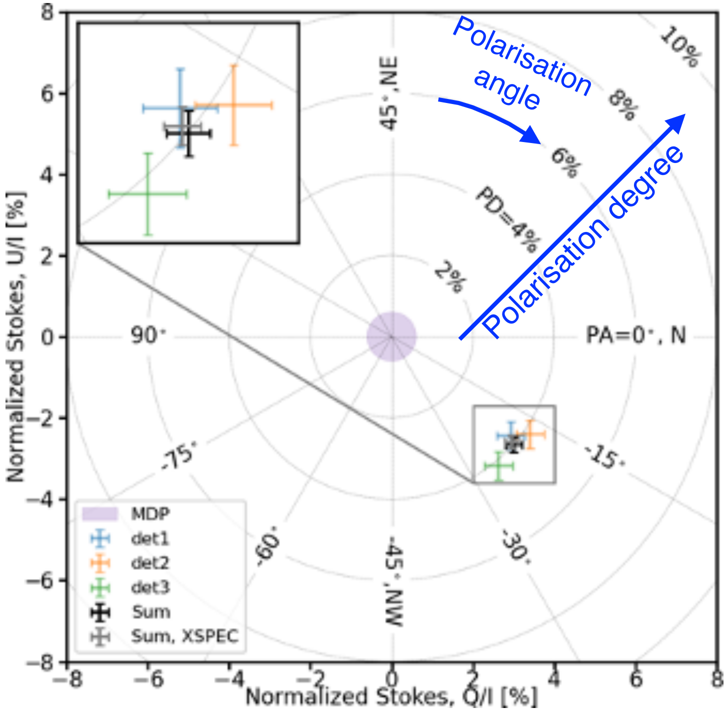

Krawczynski et al. (2022)

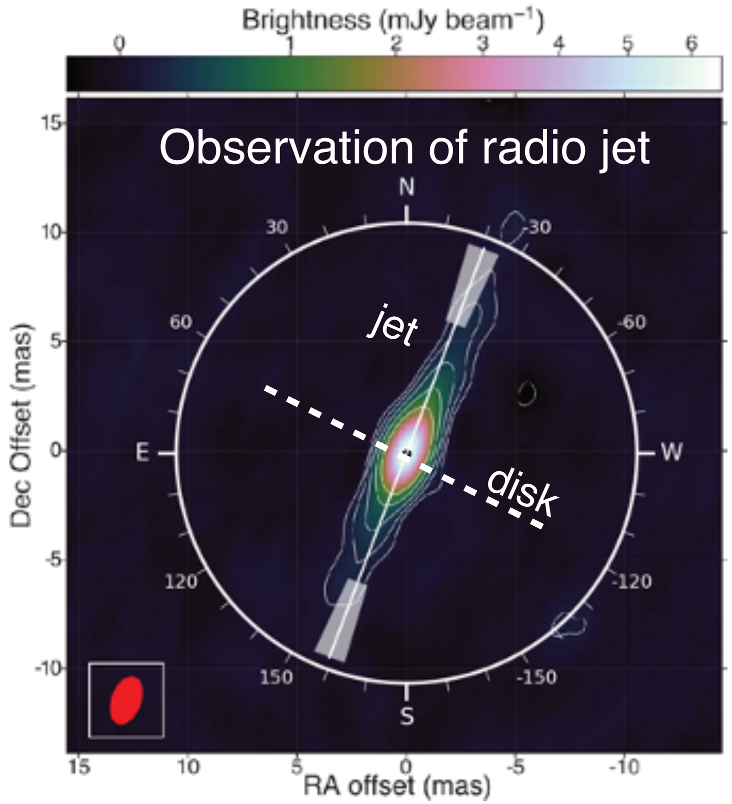

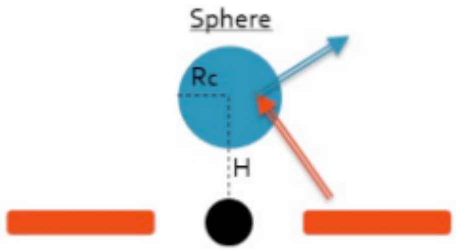

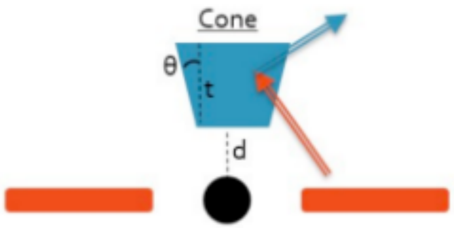

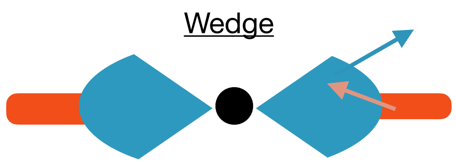

The Case of the Microquasar Cygnus X-1

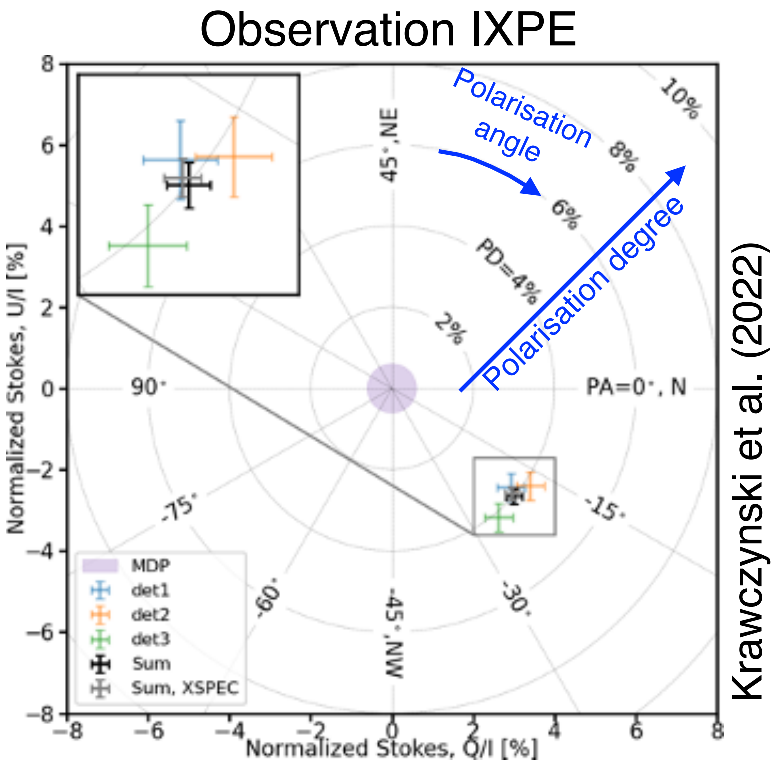

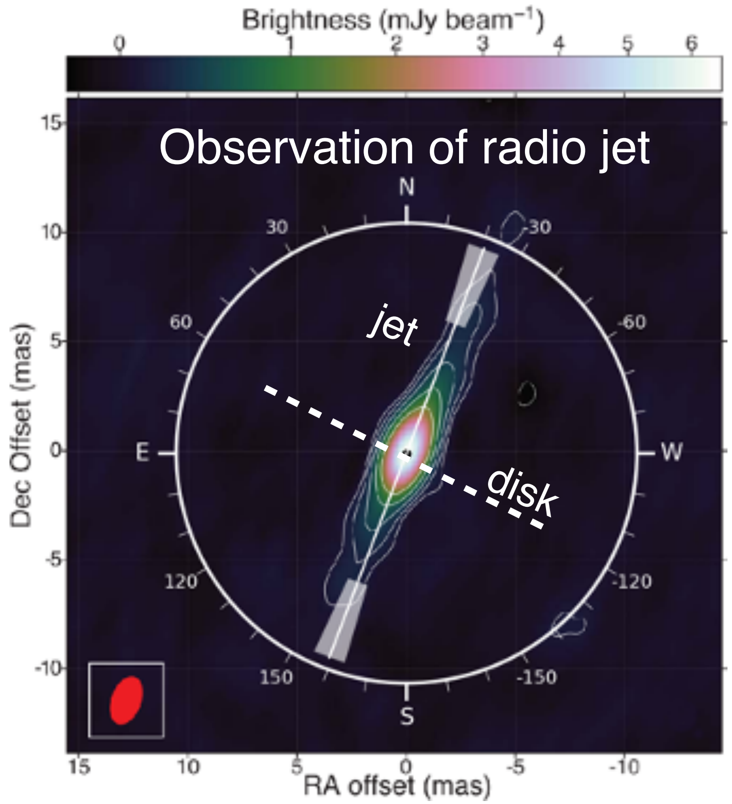

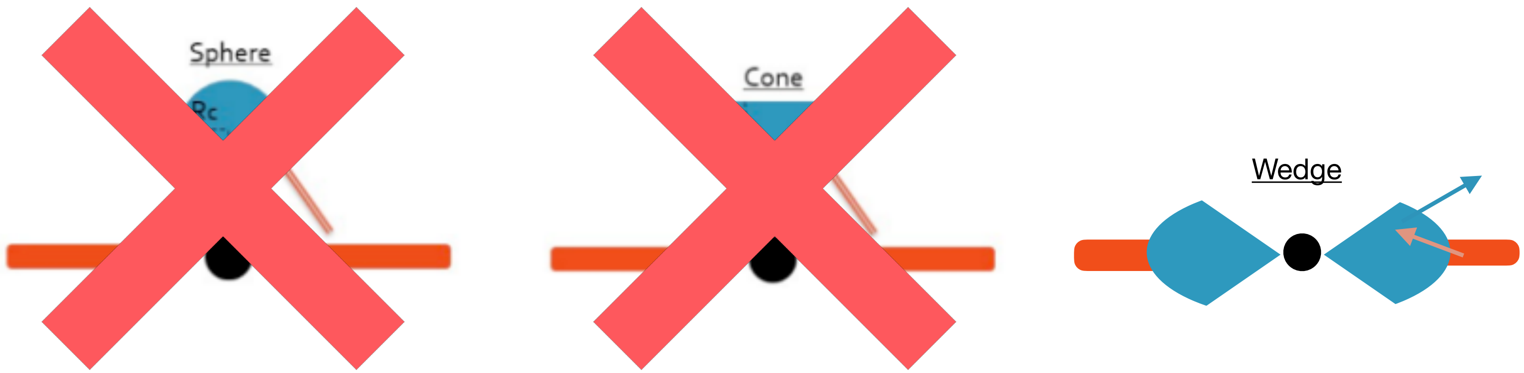

The Case of the Microquasar Cygnus X-1

Observation IXPE

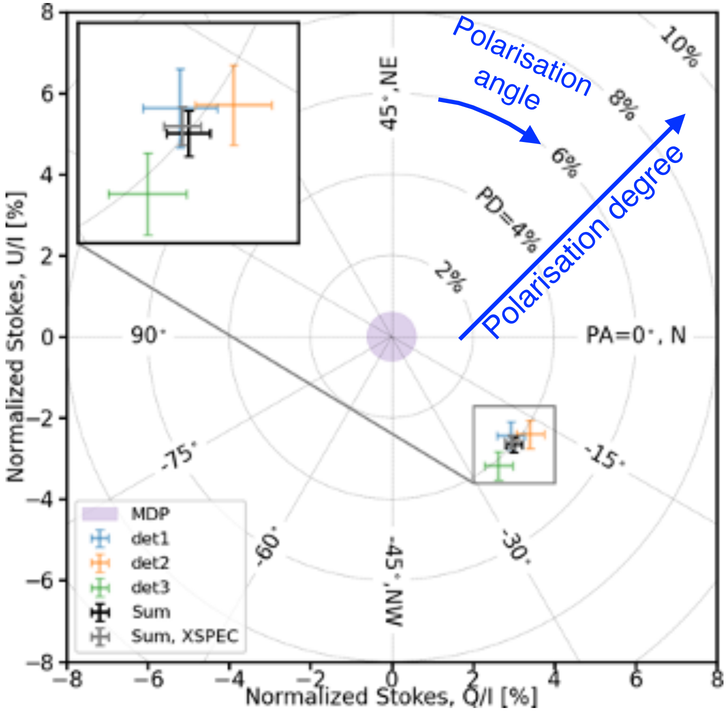

Krawczynski et al. (2022)

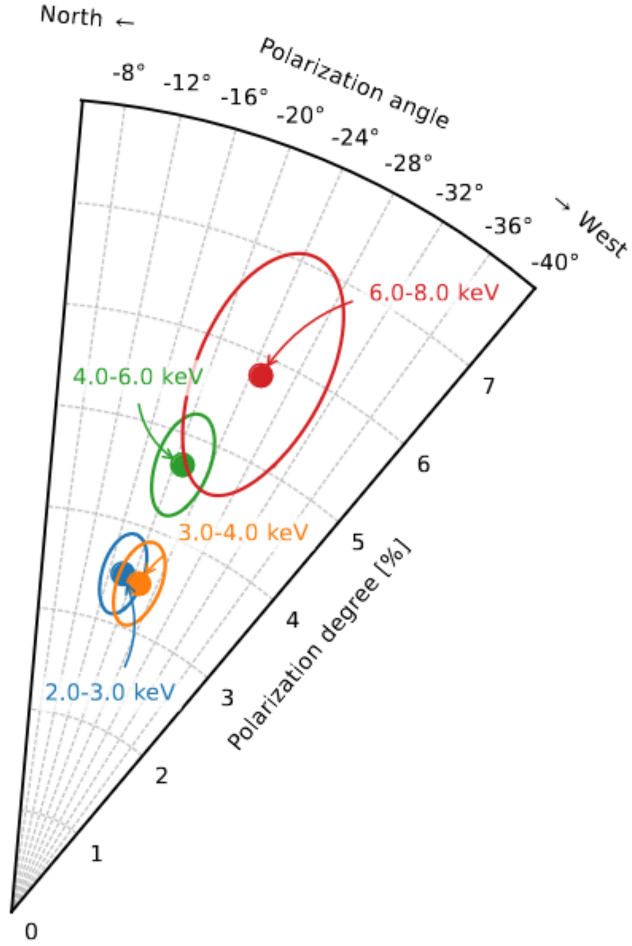

BUT:

•Too large polarisation degree (4% instead of expected 2%)

• Polarisation increase with energy

Still not explained!!!

The Case of the AGN NGC 4151

NGC 4151 observed by IXPE

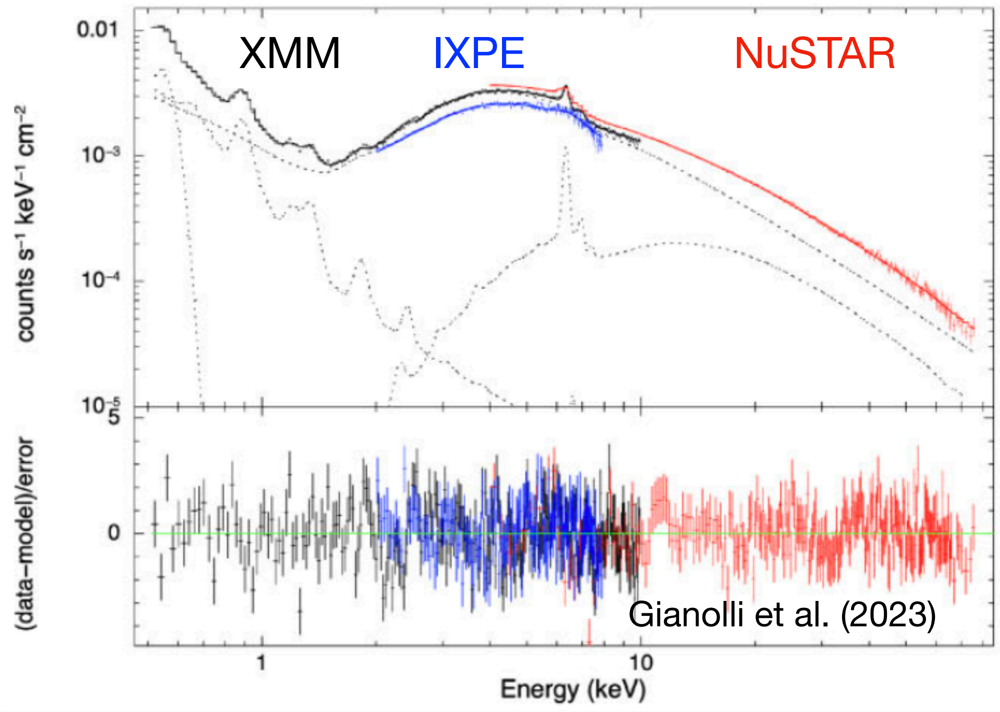

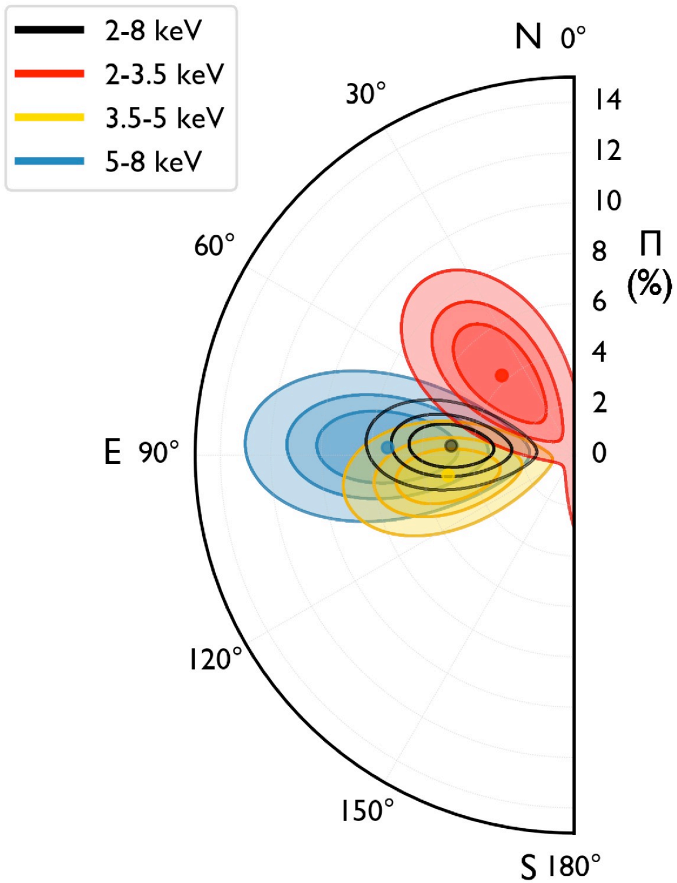

The Case of the AGN NGC 4151

NGC 4151 observed by IXPE

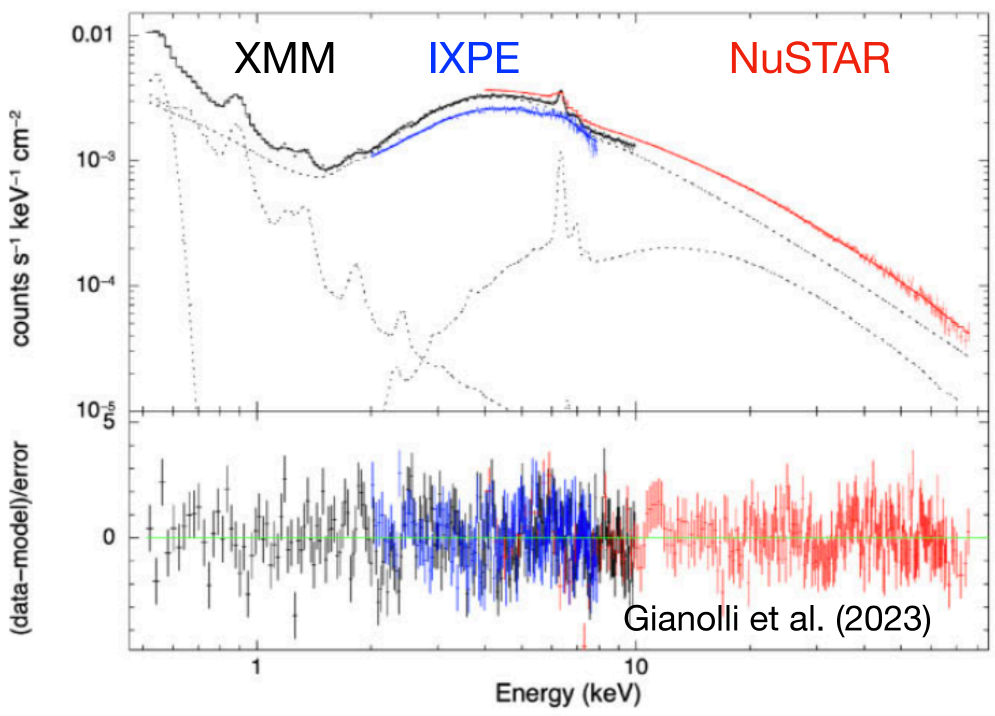

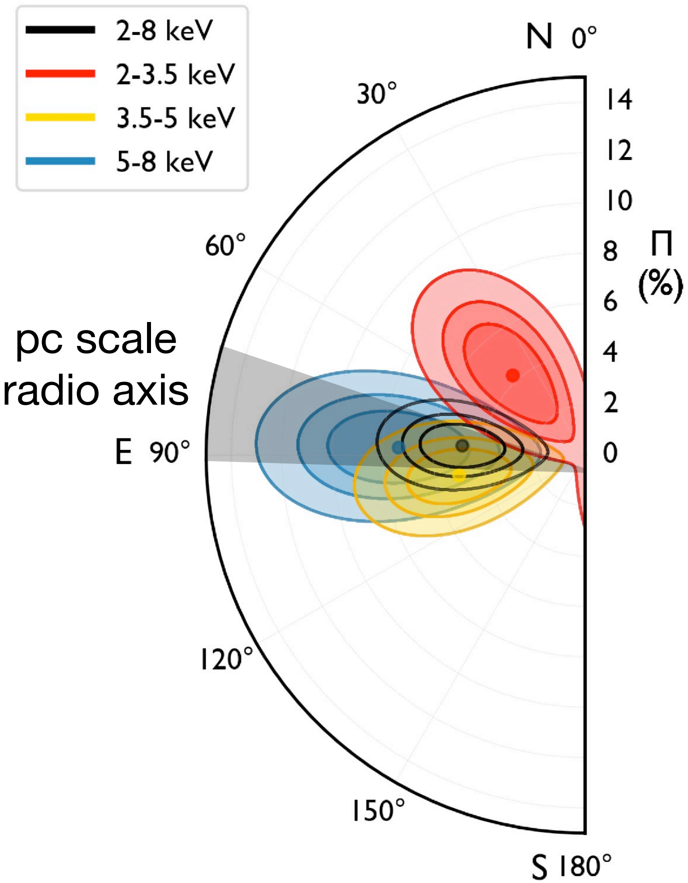

The Case of the AGN NGC 4151

NGC 4151 observed by IXPE

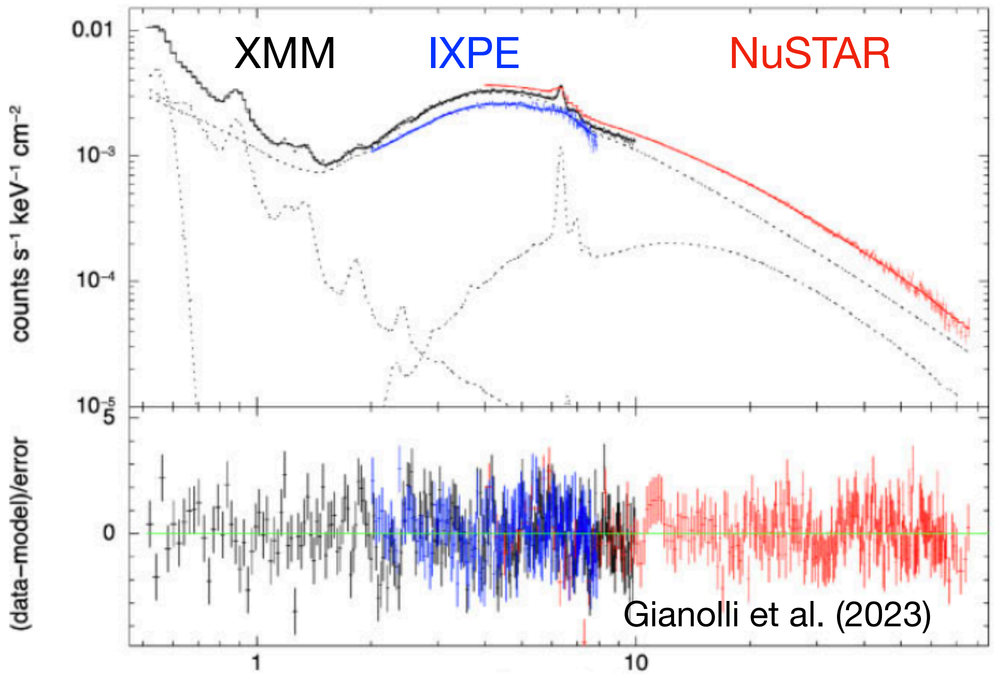

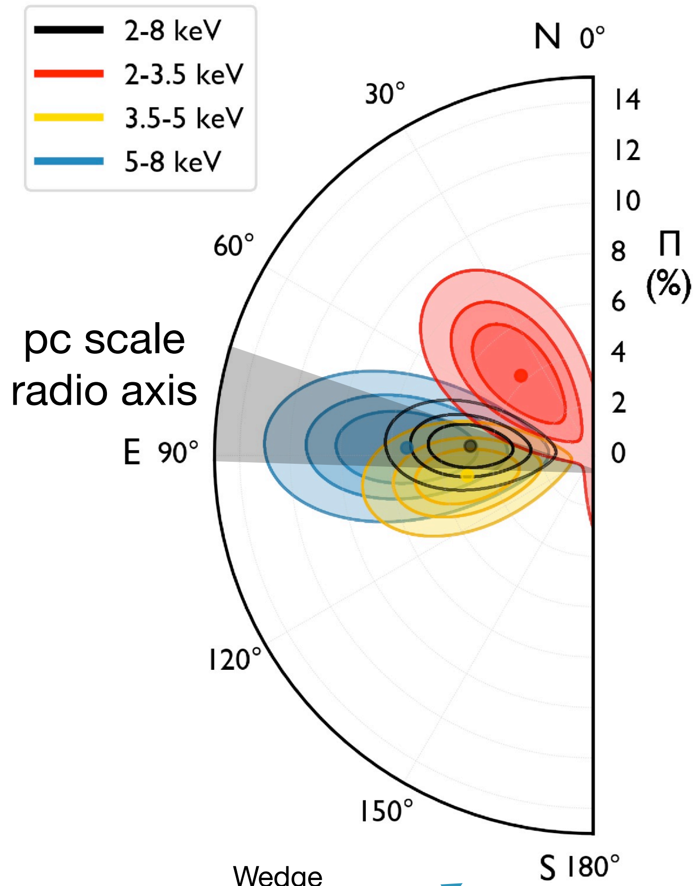

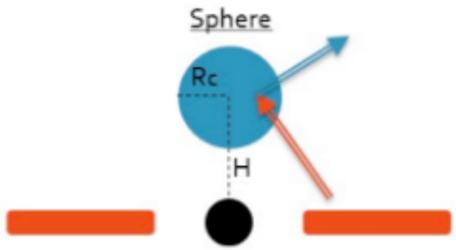

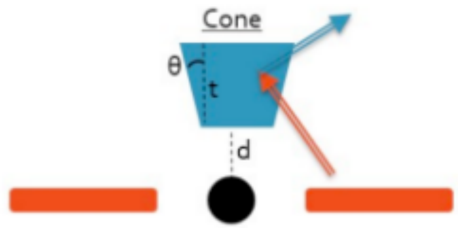

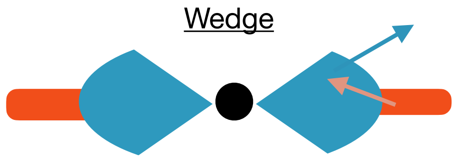

The Case of the AGN NGC 4151

NGC 4151 observed by IXPE

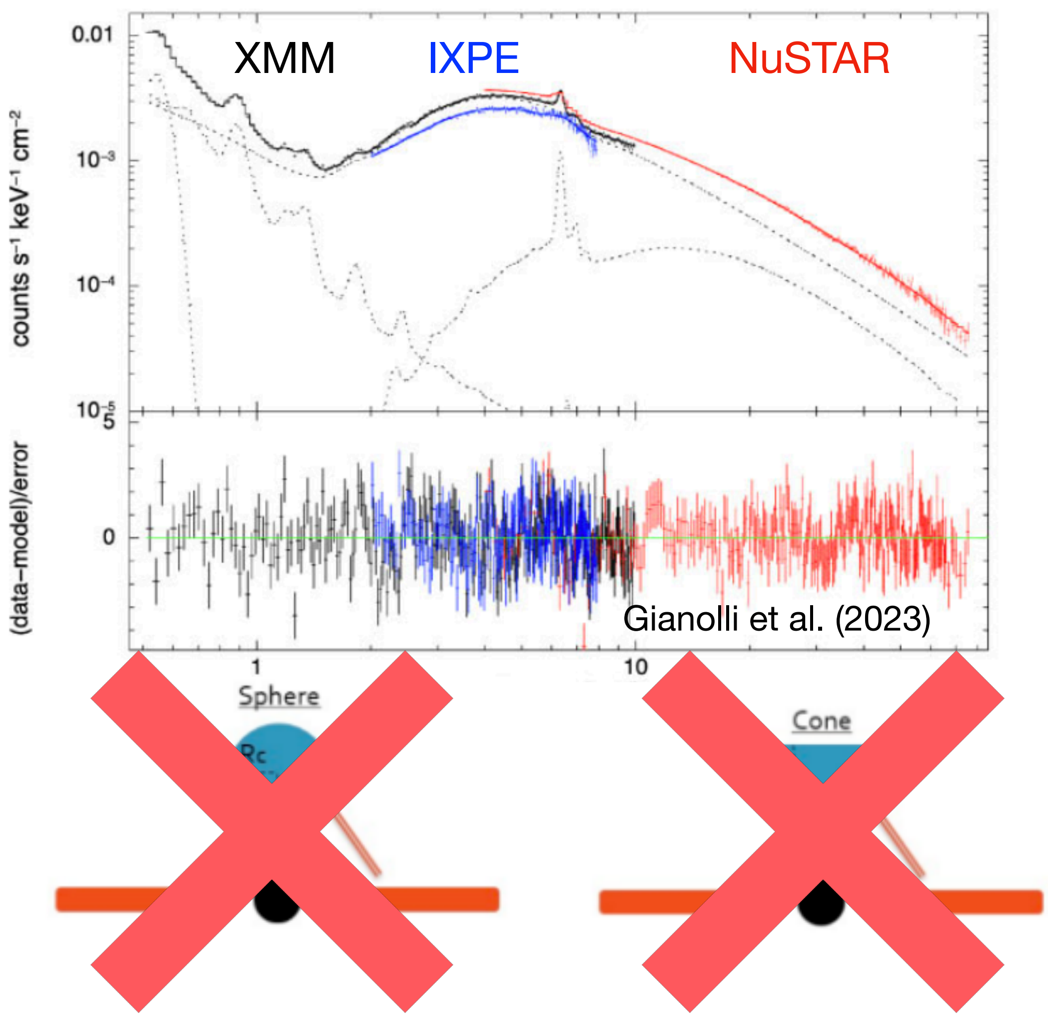

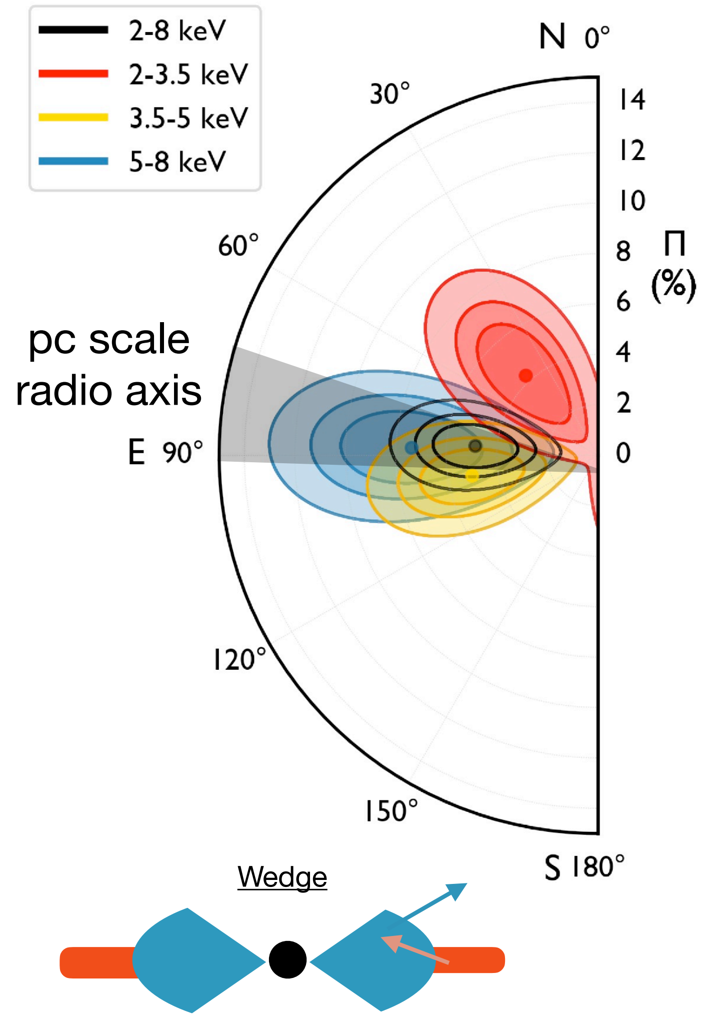

Jets in RL AGN

- 10% of AGN are radio loud and show large scale jets
- Jets production requires a large scale magnetic field threading the accretion disk   Beckwith et al. (2008)
- Different jet flavours :

Blandford & Znajek (BZ)

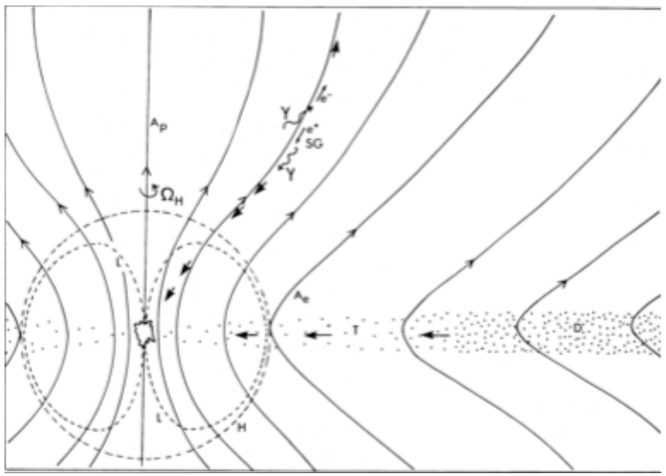

Extraction from BH rotation
Matter content: rather pairs…

Blandford & Payne (PB)

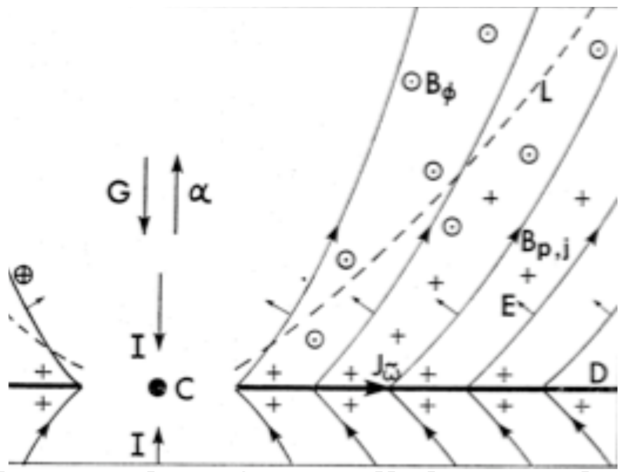

Extraction from disk rotation
Matter content: rather e⁻ / p

Jets in RL AGN

- Both observed in GRMHD…

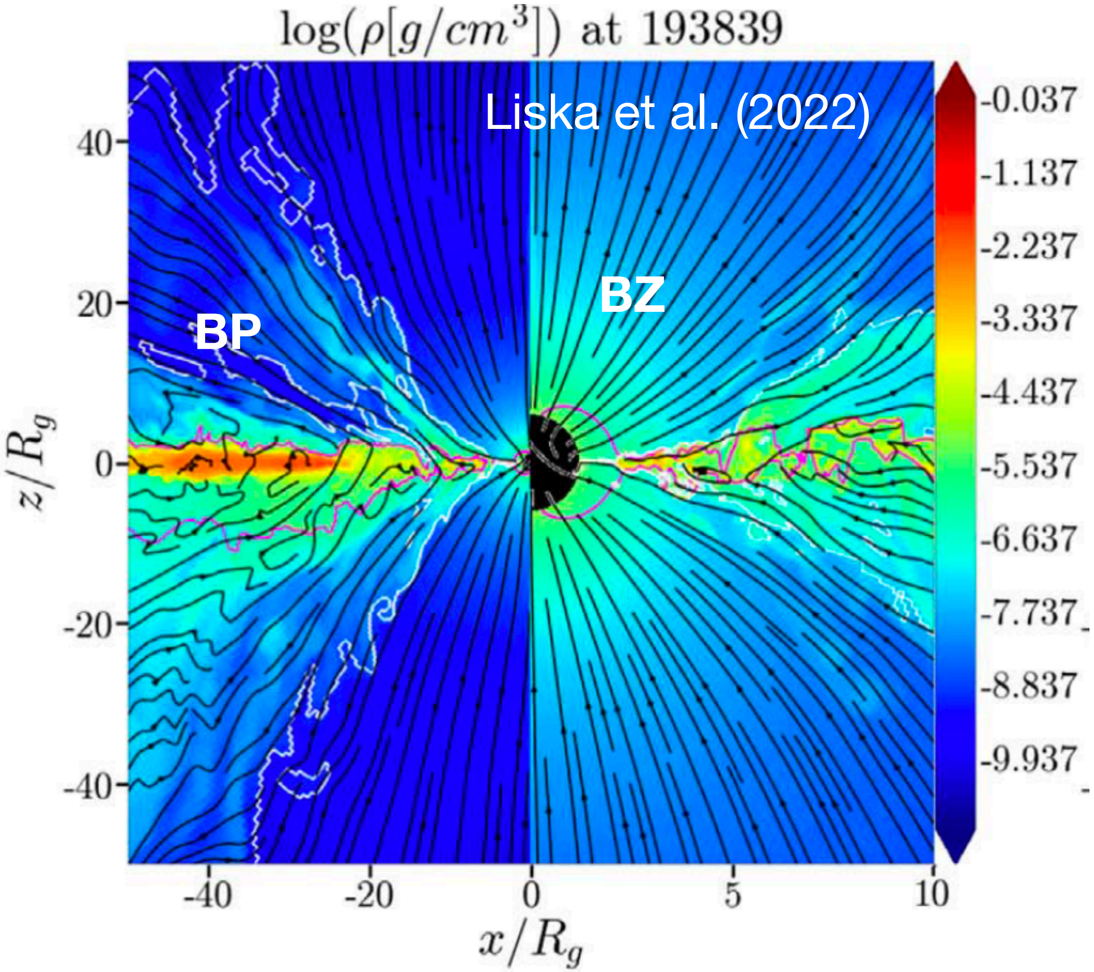

…. but which one is radiatively dominating?

Jets in Blazars

Constraints from X-ray polarisation

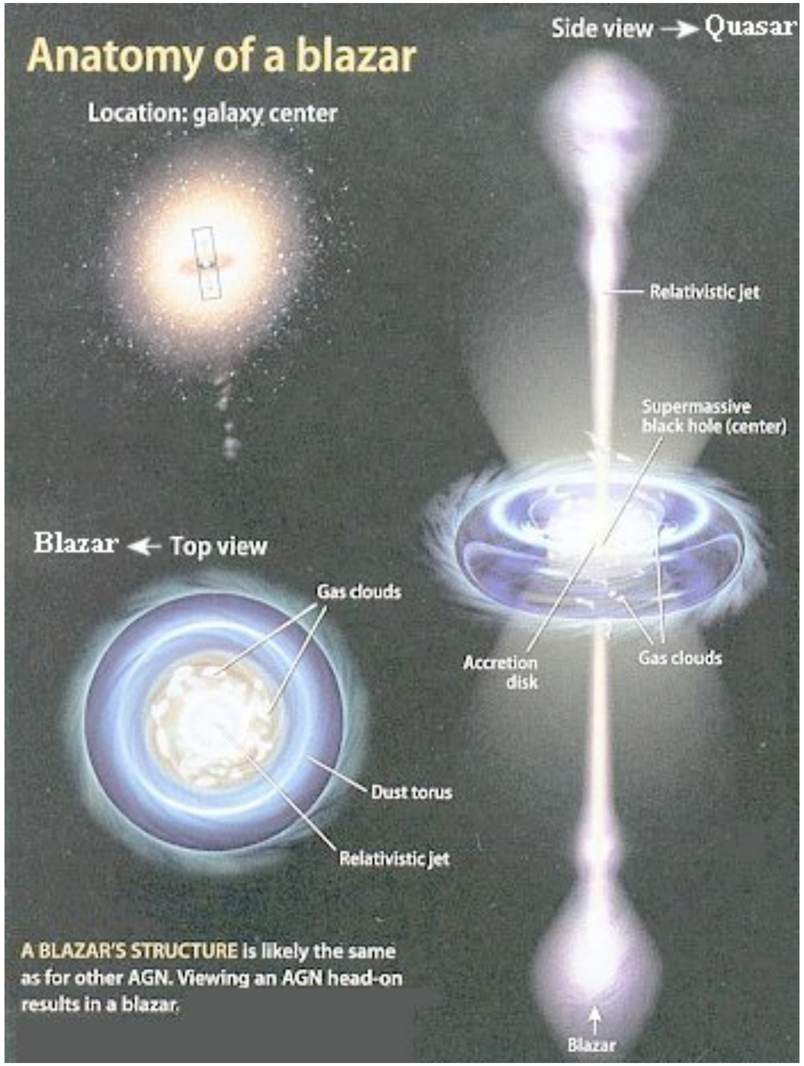

- Blazar = jetted AGN seen along the jet axis
- Blazar SED dominated by a Synchrotron and Compton component
- High Synchrotron Peak Blazar are good candidate for X-ray polarimetry (Di Gesu et al. 2022, Liodakis et al. 2022)

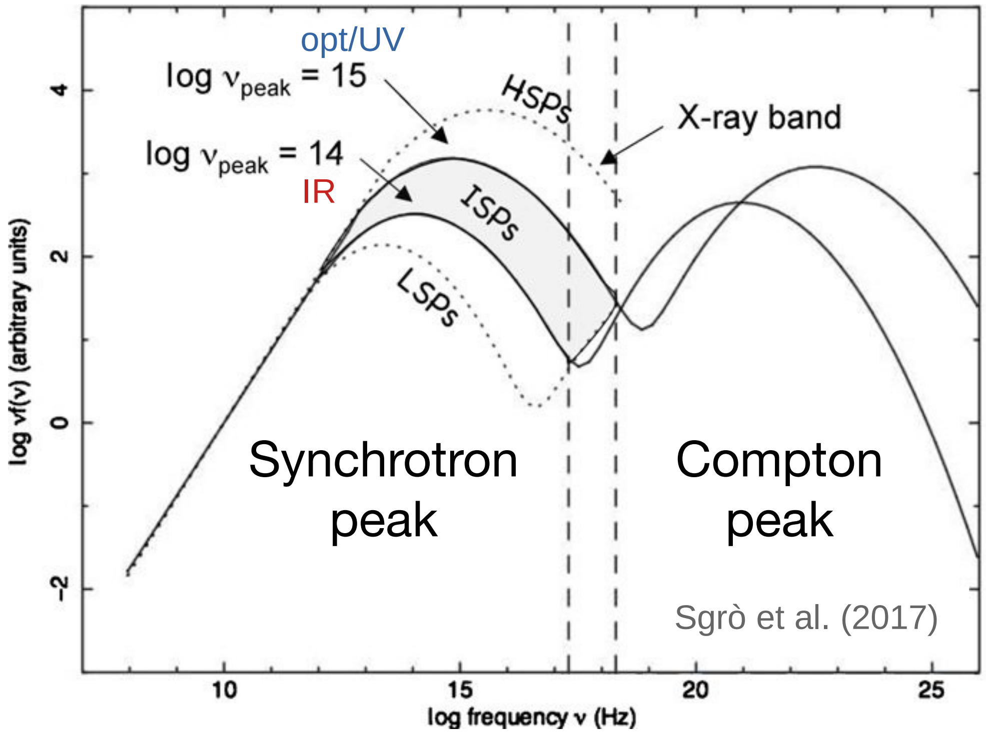

Jets in Blazars

Constraints from X-ray polarisation

Liodakis et al. (2022)

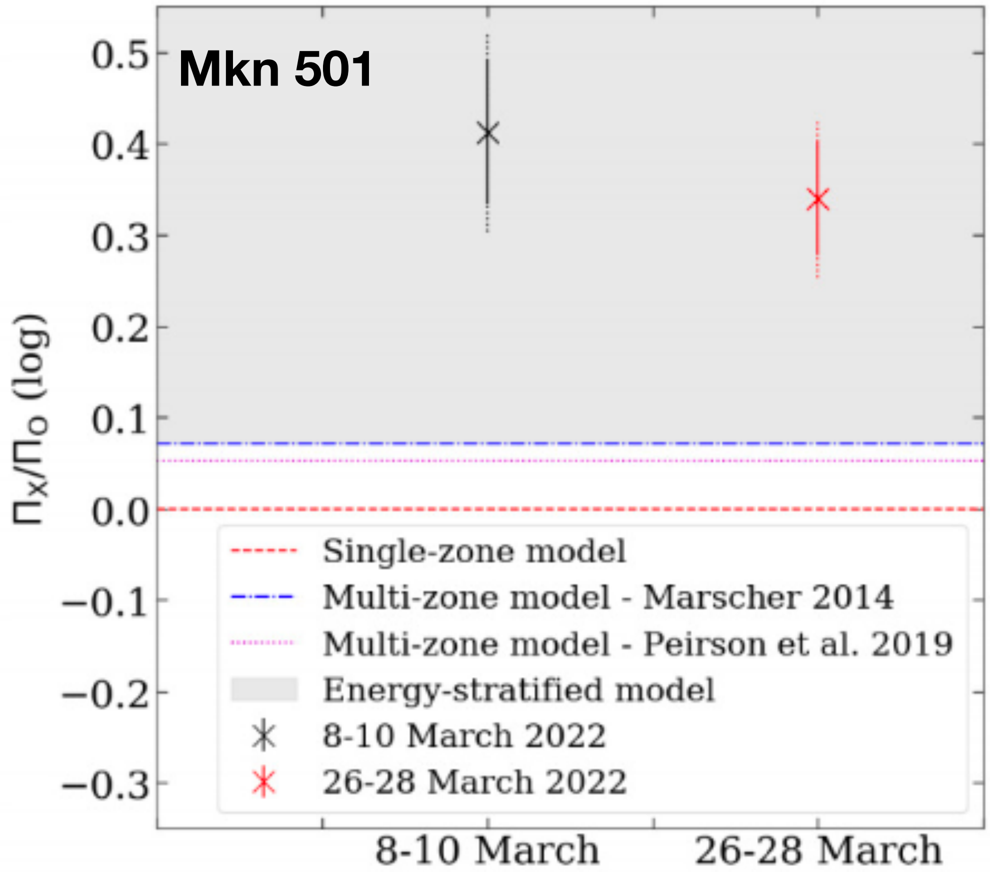

- In agreement with « energy stratified » model

➡ particles energized at a shock front and lose energy to radiation as they travel away from the acceleration site.

Jets in Blazars

Constraints from X-ray polarisation

Di Gesu et al. (2023)

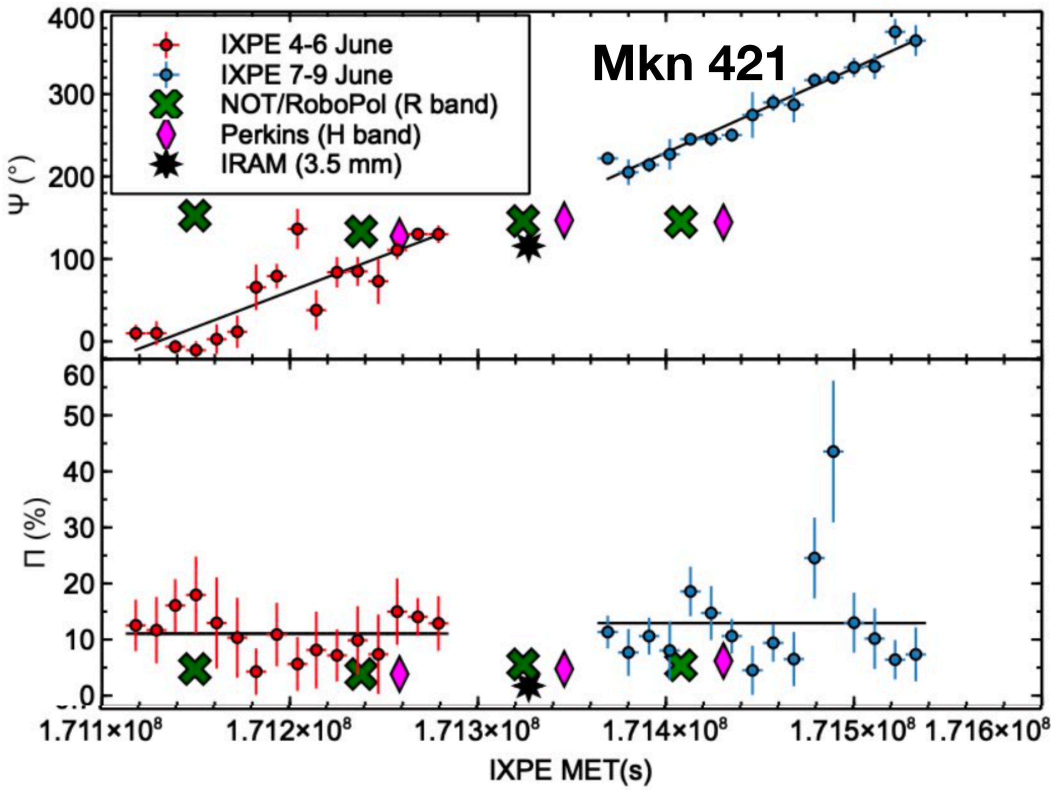

- Rotation of the polarisation angle

→ localized shock propagating along the helical magnetic structure in the jet

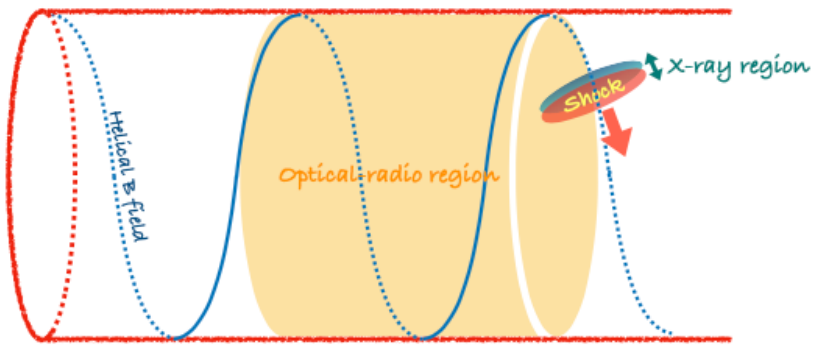

Jets in Blazars

Constraints from X-ray polarisation

Di Gesu et al. (2023)

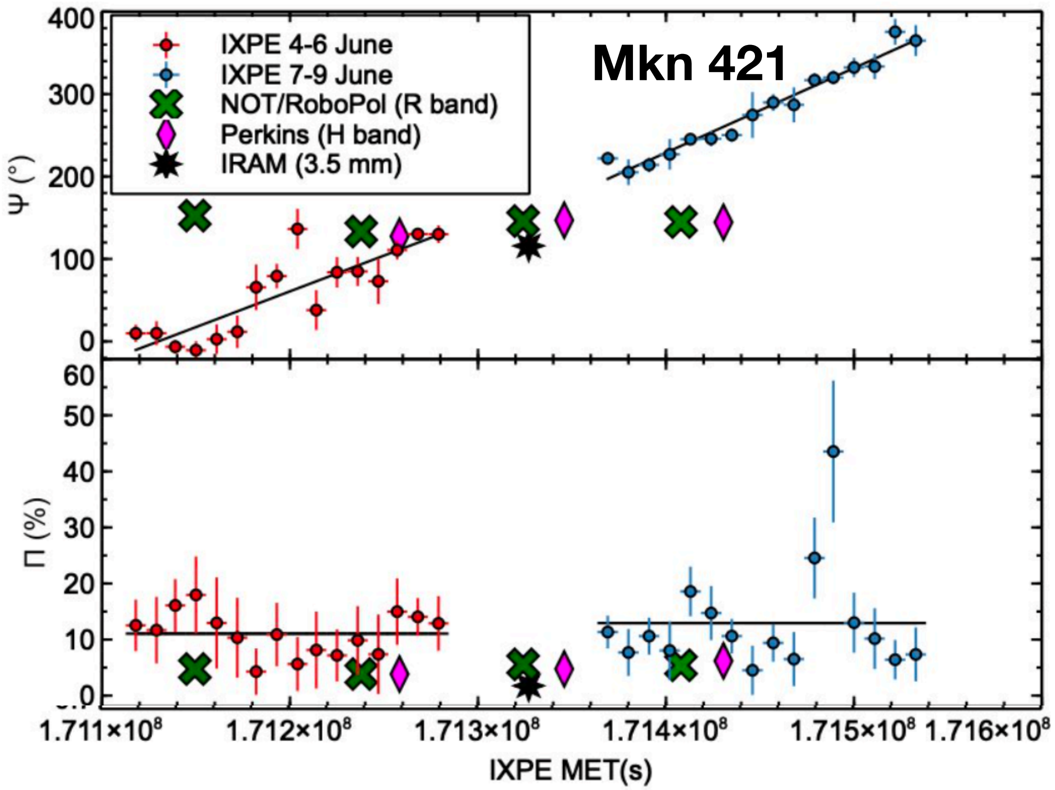

- Rotation of the polarisation angle

➡ localized shock propagating along the helical magnetic structure in the jet

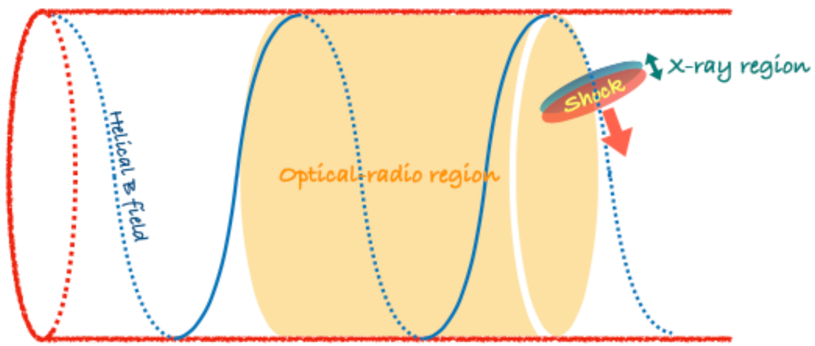

New Results to come! Stay Tune!

Thanks!